LEAF PHOTOSYNTHESIS IN WHEAT (*Triticum* spp.) UNDER CONDITIONS OF LOW TEMPERATURE AND CO_2 ENRICHMENT

A Thesis Submitted to the College of
Graduate Studies and Research
in Partial Fulfillment of the Requirements
for the Degree of Master of Science
in the Department of Biochemistry
University of Saskatchewan
Saskatoon

By
Cody J. Chytyk

PERMISSION TO USE

In presenting this thesis in partial fulfillment of the requirements for a Postgraduate degree from the University of Saskatchewan, I agree that the Libraries of this University may make it freely for inspection. I further agree that permission for copying of this thesis in any manner, in whole or in part, for scholarly purposes may be granted by the professor or professors who supervised my thesis work, or, in their absence, by the Head of the Department or the Dean of the College in which my thesis work was done. It is understood that any copying or publication on used if this thesis of parts thereof for financial gain shall not be allowed without my written permission. It is also understood that due recognition shall be given to me and to the University of Saskatchewan in any scholarly use which may be made of any material in my thesis.

Requests for permission to copy or to make use of materials in this thesis in whole or in part should be addressed to:

Head of the Department of Biochemistry
University of Saskatchewan
107 Wiggins Road
Saskatoon, Saskatchewan
S7N 5E5 CANADA

ABSTRACT

It is well known that photosynthetic health impacts the overall fitness of the mature plant. This study aims to determine photosynthetic vigour of spring wheat cultivars during field development as well as their biomass composition at maturity to determine which cultivars/varieties would be optimum for cellulosic ethanol production. Additionally, specimens were grown at non-acclimating (20˚C), cold acclimating (5˚C), non-acclimating high CO_2 (20˚C/750 µmol mol^{-1} CO_2) and cold-acclimating high CO_2 (5˚C/750 µmol mol^{-1} CO_2) to resolve photosynthetic responses to different environments. Plants were photoinhibited under high irradiance (5 fold growth irradiance) and low temperature (5˚C) while photochemical efficiency of PSII was monitored throughout using chlorophyll fluorescence imaging. Vegetative production was monitored using normalised difference vegetation index. De-epoxidation of xanthophyll photoprotective pigments were also recorded using HPLC and photochemical reflectance index. Additionally, carbon assimilation rate was recorded with infra-red gas analysis methods. It was discovered that no one wheat cultivar demonstrated any photosynthetic advantage in the field or under photoinhibitory conditions. However, photosynthetic differences were observed between wheat grown in different environments. Plants that were cold-acclimated or grown under high CO_2 were more resilient to photoinhibitory stress. This was also reflected by most cold-acclimated cultivars having increased triose phosphate utilization, electron transport and zeaxanthin induction. Plants acclimated to high CO_2 at room temperature also displayed increased electron transport and triose phosphate utilization but had decreased zeaxanthin induction. It is hypothesized increased excitation pressure in cold acclimated and high CO_2 cultivars allowed for their increase in the development of photoinhibitory tolerance.

ACKNOWLEDGEMENTS

I would like to express my most sincere thanks to Dr. Gordon R. Gray for his scientific guidance, opinions and financial support.

I would also like to express gratitude to members of my graduate committee: Dr. Todd, Dr. Warrington and Dr. Khandelwal for their time and patience in the completion of this thesis.

A special thanks to Dr. Pierre Hucl for allowing me to use plants from his varietal trial in 2007 and 2008 and for procuring seed for chamber studies. Kenneth Jackie and Mike Grieman also deserve recognition for they were instrumental in the success of my field experiments.

Thanks also to Dr. Norman Huner and his students, Keshav Dahal and Rainier Bode for assistance with their laboratory equipment in London.

My former lab members Nitya Khanal, Sarah Klatt, Ze Long Lim, Pawel Brzezowski, Denise Broersma, Anita Agblor and John David Mckinnon proved extremely valuable throughout the years. Thanks for the help and ambition.

My parents also deserve credit for helping me financially and mentally throughout my academic life. Thanks!

Most importantly, my girlfriend Kate was with me my entire graduate career and was patient and loving throughout. Thanks for all the support.

TABLE OF CONTENTS

Page

LIST OF TABLES

LIST OF FIGURES

LIST OF ABBREVIATIONS

Abbreviation	
ϕ_a	CO_2 apparent maximum quantum yield of CO_2 assimilation
Γ	CO_2 compensation point
A	antheraxanthin
A	rate of leaf carbon assimilation
ATP	adenosine triphosphate
A/C_i	CO_2-response curve
A/Q	light-response curve
A_{max}	maximal rate of leaf carbon assimilation (at saturating CO_2 or irradiance)
β-C	beta-carotene
C_a	ambient CO_2 partial pressure
CE	leaf carboxylation efficiency
Chl	chlorophyll
C_i	intercellular CO_2 partial pressure;
DW	dry weight
E	transpiration rate
EPS	epoxidation state
F	fluorescence emission
FNR	ferredoxin-NADP oxidoreductase
F_M	maximal fluorescence in the light-adapted state
F_O	background fluorescence in the dark-adapted state
F_V	variable fluorescence (F_M-F_O);
F_V/F_M	((F_M-F_O)/F_M), photochemical efficiency of PSII
FW	fresh weight
g_s	stomatal conductance to water
HPLC	high-performance liquid chromatography
I_a	absorbed light flux
IRGA	infra-red gas analysis
J_{max}	electron transport rate

k_P	constant for rate of photochemistry
k_D	constant for rate of thermal deactivation
k_T	constant for rate of excitation energy transfer
k_F	constant for rate of fluorescence emission
L	lutein
LHC	light harvesting complex
N	neoxanthin
NDVI	normalized difference vegetation index
NIR	near-infrared radiation
NPQ	non-photochemical quenching
PPFD	photosynthetic photon flux density
PRI	photochemical reflectance index
PSI	photosystem I
PSII	photosystem II
PQ	plastoquinone
Q	irradiance
Q_A	first quinone acceptor
Q_B	second quinone acceptor
R_1	dark respiration
Resp	sum of dark and light respiratory processes
SRI	spectral reflectance indices
T_{air}	air temperature
T_{leaf}	leaf temperature
TLC	thin-layer chromatography
TPU	triose phosphate utilisation
V	violaxanthin
$V_{c,max}$	carboxylation rate
VIS	visible
vpdL	leaf to air vapour pressure difference (calculated from T_{leaf})
WUE (A/E)	intrinsic water use efficiency
Z	zeaxanthin

1.0 INTRODUCTION

This study aims to investigate the photosynthetic properties of commonly-grown western-Canadian wheat varieties on the basis of their acclimatory and photoinhibitory responses to abiotic stress. Wheat plants were sown in field conditions, low-temperature, high light and high concentrations of CO_2. Photosynthetic responses are among the most dynamic in nature and by observing photoinhibitory stress one can make deductions about photosynthetic fitness. The findings of these studies are mainly intended to elucidate the effects that high CO_2 (current climate change estimates) will have on C_3 photosynthetic plants (Zeng *et al.,* 2004). Additionally, photosynthesis of field grown wheat will also be characterised and compared to that of controlled environment chambers. Photosynthesis has been shown to be flexible, adjustable and a primary sensor to plant stress responses (Ensminger *et al.*, 2006). Since photosynthesis is the elementary process of life, the author believes it a topic worthy of further study.

Past research on photoinhibitory stress in field wheat has mainly focused on drought/high temperature stress (Yang *et al*., 2006) and diurnal changes (Lu *et al*., 2001). Few studies have particularly focused on comparing field-grown wheat to that grown in the chamber. Clearly, field-grown wheat undergoes continuous photosynthetic stress due to fluctuating temperature, humidity, water availability, nutrition and irradiance. Wheat grown under these conditions could have increased tolerance to photoinhibition and in essence, could be “field-acclimated”.

Previous studies on C_3 plants grown under high CO_2 concentrations (500-750 µmol mol^{-1}) have shown increased tolerance to photoinhibition. Electron transport rates and overall photosynthesis has been shown to increase when developed at high CO_2 (Hymus *et al*., 2001a, 2001b). Activities of Calvin cycle enzymes has also been shown to increase when grown under high CO_2 (Ainsworth and Long, 2005; Alosnso *et al*., 2009) as well as an increase in light harvesting complex absorptive cross section. (Gutiérrez *et al*., 2009). Water use efficiency has also been shown to increase (Ainsworth and Long, 2005). These factors have allowed plants when grown at high CO_2 to have more efficient photosynthesis and accumulate more biomass (Harley *et al*., 1992).

The objectives of this thesis are:

1) To study photosynthesis (carbon assimilation rate, NDVI) of spring wheat grown in a field environment as well as responses to photoinhibition (PRI, xanthophyll induction,

F_V/F_M).

2) To determine biomass characteristics (root:shoot, DW, composition) of field-grown wheat.
3) To study photosynthetic and photoinhibitory responses of spring and winter wheat grown in controlled environmental chambers at non-acclimating, cold-acclimating and high (750 μmol mol^{-1}) CO_2.
4) To determine what growth regime results in increased photoinhibitory tolerance, photosynthetic rates and hypothesize an explanation.

2.0 LITERATURE REVIEW

2.1 Photosynthesis

All life forms on earth consist of carbon that was once assimilated from atmospheric CO_2 by photosynthesis. Photosynthesis is an elaborate process by which plants convert sunlight into usable chemical energy. This process takes place in the thylakoid membrane in the chloroplast of higher plant cells (Ensminger *et al*., 2006).

The reactions of photosynthesis are initiated when the antenna complexes of photosystem I (PSI) and photosystem II (PSII) captures sunlight (Krause and Weis, 1991). Here, two types of chlorophyll (Chl) molecules, Chl *a* and Chl *b* absorb the excitation energy of the sunlight. The Chl molecules are held in proper orientation by a large number of proteins in the light harvesting complex (Malkin and Niyogi, 2000). The excitation energy absorbed by the antennae is then transferred to the reaction centers of both photosystems where it enters the photosynthetic electron transport chain in the thylakoid membrane.

The PSII reaction center multi-subunit complex is integral in the thylakoid membrane. The PSII complex has a specific set of Chl molecules referred to as P680 (Krause and Weis, 1991). The excitation energy from the sunlight is enough to cause charge separation in the PSII reaction center and water donates an electron to pheophytin *a* via the oxygen evolving complex and chlorophyll P680 (Fig 2.1). The electron is then transferred to the first stable quinone acceptor (Q_A). Q_A can then reduce the second quinone acceptor, Q_B. The quinones can accept another electron which causes two protons to associate with Q_B and become a Q_BH_2 molecule (Malkin and Niyogi, 2000). This molecule then leaves PSII to the thylakoid membrane. Here, it associates with cytochrome b_6/f protein complex. Cytochrome b_6/f aids in the transfer of electrons to plastocyanin which releases the protons. Cytochrome b_6/f ensures the protons from Q_BH_2 are released into the lumen. An ATP synthase complex then pumps the protons back into the stroma in a process which produces ATP (Malkin and Niyogi, 2000).

The PSI reaction center resembles PSII but has different reaction center chlorophylls known as P700 (Malkin and Niyogi, 2000). The reduced plastocyanin is able to bind the PSI and the absorbed excitation energy by the PSI antenna transfers electrons from plastocyanin to ferredoxin. Upon reduction, ferredoxin is released from PSI and interacts with ferredoxin-NADP oxidoreductase (FNR). FNR contains a flavonoid adenine dinucleotide molecule (FAD). FAD is

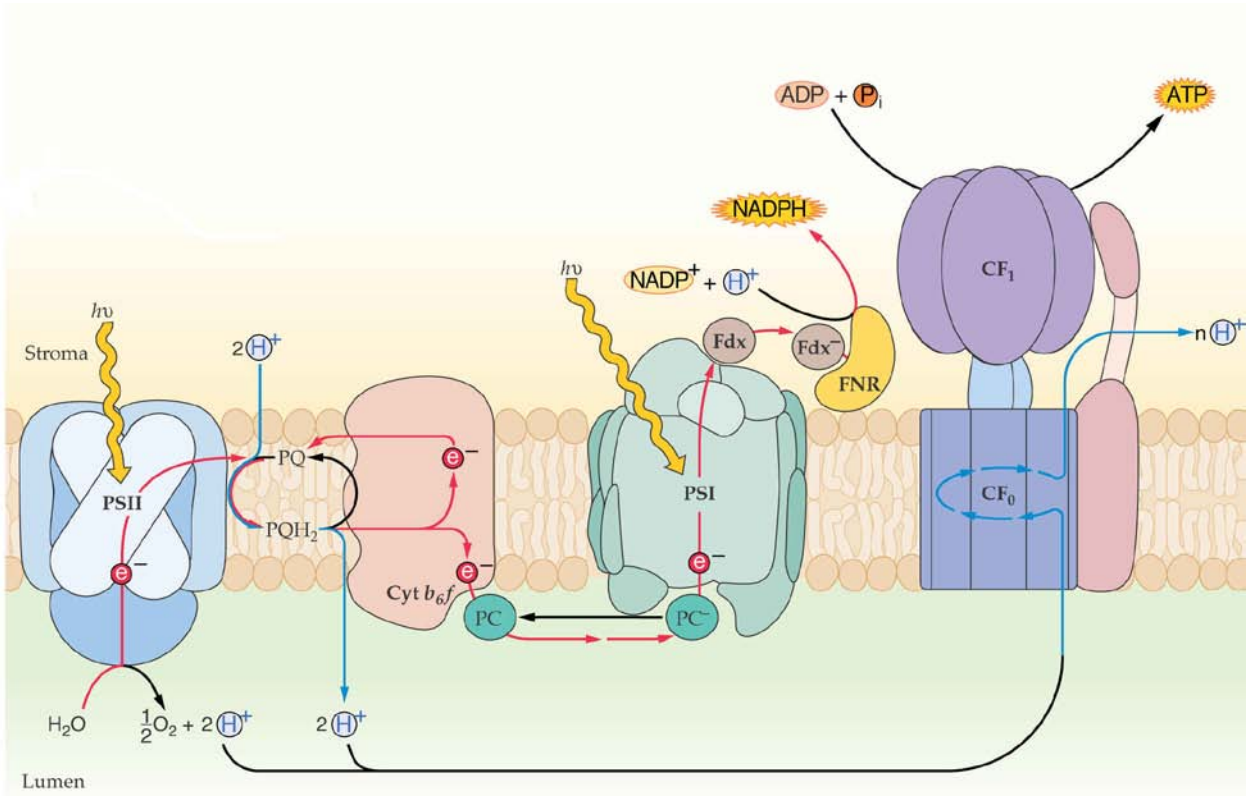

Figure 2.1 Light reactions of photosynthesis. Incoming irradiance energy is represented by "*hv*".

then able to reduce NADP to NADPH.

The ATP and NADPH produced in the chloroplast are the energy used by the enzymes of the Calvin cycle to produce carbohydrates (Nelson and Cox, 2005, Fig 2.2). In C_3 plants, ribulose 1,5-bisphosphate carboxylase/oxygenase (Rubisco) fixes a CO_2 molecule and combines it with one ribulose 1,5-bisphosphate molecule to produce two molecules of 3-phosphoglycerate. The 3-phosphoglycerate is then converted to 1,3-bisphosphoglycerate by 3-phosphoglycerate kinase, using ATP as the phosphoryl donor. NADPH reduces 1,3-bisphosphoglycerate into glyceraldehyde 3-phosphate and is catalyzed by glyceraldehyde 3-phosphate dehydrogenase. Triose phosphate isomerase then converts glyceraldehyde 3-phosphate into dihydroxyacetone phosphate. Most of the triose phosphate produced is put back into the Calvin cycle as ribulose 1,5 bisphosphate or exported to the cytosol for sucrose biosynthesis. The rest is retained in the chloroplast for starch synthesis. Under optimal conditions, ATP and NADPH formed during the light reactions are efficiently and completely used by the dark reactions of photosynthesis. This scenario is referred to as photostasis and is necessary for plant fitness.

2.2 Photoinhibition and photoprotection

Photoinhibition is the reversible decrease of photosynthesis during stressful photosynthetic conditions. More commonly, photoinhibition occurs when low temperature or high irradiance decrease the rates of photosynthetic activity and photosynthetic efficiency of PSII (Gray *et al*., 2003). The rates of the metabolic reactions of the Calvin cycle are severely decreased at low temperature whereas the light reactions are less affected by temperature (Huner *et al*., 1998). Because the light reactions can take place at a faster rate than the dark reactions, more excitation energy is harnessed than can be used for carbon uptake. An intricate balance must be maintained between these processes to ensure that the ATP and NADPH produced by the photochemical reactions are not in excess or oxidative damage could result. If $NADP^+$ is not available in high enough concentrations, O_2 will be reduced instead and reactive oxygen species will form. To avoid this potential energy crisis, the plant modulates photosynthetic control in an attempt to achieve photostasis (Holt, 2005; Ensminger, 2006). Upon placement into low temperature or high light, sucrose biosynthesis is decreased (Savitch *et al*., 1997). After hours of decreased sucrose synthesis, accumulation of phosphorylated carbon intermediates ensues due to their decreased transport (Strand *et al.*, 1997; Stitt and Hurry, 2002). This leads to either

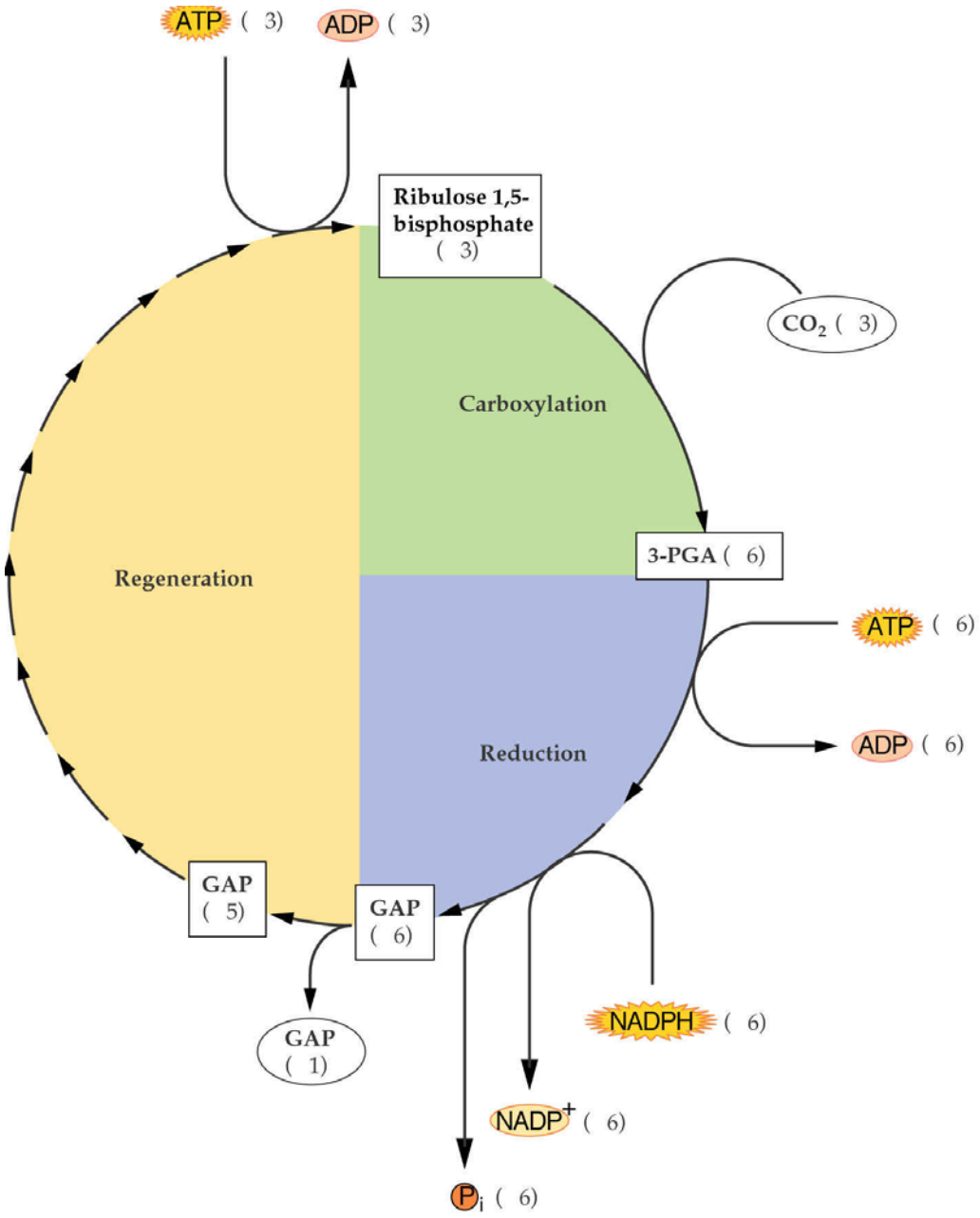

Fig 2.2. Dark reactions (Calvin cycle) of photosynthesis. Shown are the major stages: carboxylation (CO_2 is assimilation), reduction (NADPH and ATP from electron transport chain are used to reduce carbon) and regeneration of ribulose 1,5-bisphosphate.

feedback inhibition of electron transport and increased capacity for carbon metabolism (Somersalo and Krause, 1990). This is one strategy plants to use to adjust to energy imbalance in order to re-establish photosynthesis.

Early research indicated photoinhibition results in reduction of the D1 protein integral for PSII (Long and Humphries, 1994). Upon photoinhibition, immediate oxidative damage is caused to the D1 protein. This decreases the amount of excitation energy taken in and can somewhat relieve the photoinhibitory stress. Reduction in PSII antenna size is also known to directly decrease photosynthetic efficiency in this manner (Huner *et al*., 1998). More recently, Takahashi and Murata (2008) have proposed a model that views photoinhibition as a balance between damage and repair of the D1 protein. Under high light, photodamage to PSII is proportional to intensity of the incident light. The reaction center is inactivated and D1 is degraded by proteolysis. Because of the oxidative environment formed by photoinhibition, hydrogen peroxide is formed. This reactive oxygen species reduces the synthesis of D1 precursors by directly inhibiting its translation (Takahashi and Murata, 2008).

Photoinhibition is related to the oxidative state of the primary quinone acceptor, (Gray *et al.*, 1996; Sane *et al.*, 2003). Upon photoinhibition, the quinone pool now has a higher reduced state than when under photostasis due to the imbalance of metabolic reactions. This is referred to as excitation pressure. This increase in PQ reduction activates a thylakoid protein kinase which phosphorylates LHCII (Ensminger *et al*., 2006). Because of charge repulsion, LHCII prefers to associate with PSI instead of PSII. Because of this, excess excitation energy is effectively diverted from PSII. Cold acclimated winter cereals adjust their photosynthesis by having an increased oxidized Q_A pool which allows dissipation of excess light energy during photoinhibitory stress (Sane *et al*., 2003). This, in turn, increases their photoinhibitory resistance over non acclimated plants as monitored by photochemical efficiency. Cold acclimated plants have also shown an increase in intracellular inorganic phosphate concentration over non acclimated plants (Hurry *et al*., 1993). This allows for higher rates of triose phosphate utilization. Higher concentrations of inorganic phosphate in cold acclimated and phosphate-fed plants are shown to increase carbohydrate synthesis rates leading to a resistance to photoinhibition.

Photoinhibition has also been known to increase induction of the xanthophyll cycle (Demmig-Adams and Adams 1992, 1996). In this process, photoprotective pigments associate with the PSII reaction center and dissipate excess light energy as heat (Buch *et al*., 1994).

violaxanthin, is enzymatically de-epoxidized twice by violaxanthin de-epoxidase into antheraxanthin then zeaxanthin. This can only happen during photosynthetic stress as it is triggered by an acidic chloroplast lumen pH. Zeaxanthin is a photoprotectant that physically prevents excitation energy from entering the PSII reaction center. Zeaxanthin is unable to pass excitation energy to chlorophyll, effectively quenching it by releasing it as heat (Demmig-Adams and Adams, 1996). This is known as non-photochemical quenching (NPQ) and is ubiquitous in higher plant species (Demmig-Adams and Adams, 1992; Holt *et al.*, 2005). NPQ protection is readily reversible by epoxidation of zeaxanthin. Zeaxanthin has also been shown to have a role as an anti-oxidant during photoinhibitory stress (Johnson *et al*., 2007). In mutants that express three times more zeaxanthin than wild-type, photoinhibitory effects were significantly reduced without any change in NPQ. Zeaxanthin was found to bind thylakoid membranes and decrease thylakoid lipid peroxidation; a symptom of photoinhibitory stress. This evidence suggests zeaxanthin has a dual role as a photoprotectant and anti-oxidant.

Laboratory-induced high-light and low temperature photoinhibition closely resembles that which naturally-occurring plants deal with on a daily basis. It is therefore helpful to study photosynthetic responses to photoinhibition in a laboratory setting and apply it to an ecological or agricultural setting. As shown previously in this section, the most effective way to resist photoinhibition is by growth and development under high excitation pressure.

2.3 Cold and CO_2 acclimation

Acclimation refers to a phenotypic response to environmental change without any change in genetics (Huner *et al*., 1998). Cold acclimation is a process plants use to reprogram their carbon metabolism to attain photostasis and develop freezing tolerance. It usually begins with a stress response (low temperature) but eventually leads to stable, long-term adjustment in metabolism. A cold acclimated plant has grown and developed at low temperature and has metabolism different than a non acclimated plant.

As mentioned previously (section 2.2), plants have a variety of immediate responses to photoinhibition such as inactivating D1 translation, increasing quinone oxidation and induction of zeaxanthin. However, these are just temporary strategies in adjustment to low temperature and preparation for freezing temperatures. The quinone pool oxidation state is believed to be a primary sensor of photoinhibitory stress (Ensminger *et al*., 2006). Upon high excitation pressure,

a redox signal from the PQ pool regulates chloroplast and nuclear photosynthetic and cold-acclimation gene transcription (Strand *et al.*, 1997; Huner *et al.*, 1998; Hurry *et al.*, 2000; Pfannschmidt, 2003). This leads to an increase in Calvin cycle enzymes leading to higher photosynthetic capacity. Additionally, cold acclimated plants have been found to have higher activities for Calvin cycle and carbon metabolism enzymes (Hurry *et al.*, 1995; Strand *et al.*, 1999). Rubisco, phosphoglycerate kinase, Suc-6-P synthase and phosphoribulokinase have been demonstrated to have nearly 2-fold increase in activity over non acclimated plants. This, in turn, would allow for an increase in Calvin-cycle activity (phosphorylated sugar transport/utilization and ATP synthesis) under low temperatures and restoration of photostasis.

During cold-acclimation and photostasis, the plant must also restore the PSII reaction center by increasing synthesis of the D1 protein to achieve optimal photochemical yield (Ensminger *et al.*, 2006; Takahashi and Murata, 2008). Because acclimation restores favourable photosynthetic conditions, D1 is no longer damaged by reactive oxygen species and can be translated and function without hindrance.

Plants can also acclimate to grow at higher than ambient CO_2 concentrations. With current CO_2 concentrations (~380 µmol mol^{-1}) expected to double within the next century, research has been undertaken to study how plants will respond to this atmospheric change (Zeng *et al.* 2004). Some immediate benefits of growth under high CO_2 is decreased stomatal conductance leading to lower transpiration and better water use efficiency (Ainsworth and Long, 2005). In C_3 and C_4 plants, high CO_2 concentrations (600-800 µmol mol^{-1}) have been shown to increase carbohydrates and biomass (Harley *et al.*, 1992). Also, carboxylation, electron transport and photosynthetic rates increase (Alonso *et al.*, 2009). Levels of Rubisco decrease in plants grown in high CO_2. Therefore the increase in carbon assimilation is caused by an increase in substrate (CO_2) concentration for Rubisco, leading to overall higher activity and carbon fixation.

Other studies have found an inherent relation between growth at high CO_2 and photosynthetic fitness. Photochemical efficiency has been demonstrated to increase while photochemical quenching decreases in plants grown under high CO_2 (Gutierrez *et al.*, 2009). Other connections have also been made between increased electron and carboxylation rates with photoinhibitory resistance (Hymus *et al.*, 2001a, 2001b). Plants grown in increased CO_2 have increased resistance to photoinhibitory conditions leading to increased photosynthetic fitness.

2.4 Measurements of photosynthesis

2.4.1 Chlorophyll fluorescence

Chlorophyll *a* (Chl *a*) is the major pigment molecule in the PSII antenna complex. The light absorbed by this molecule is used to drive photosynthesis. However, not all light energy is absorbed is used for this process (Figure 2.3). A portion is dissipated as heat and some is re-emitted at a longer wavelength (Maxwell and Johnson, 2000). The re-emitted light is known as chlorophyll fluorescence. Since these are competing processes, chlorophyll fluorescence can be used as a reliable and non-invasive probe of photosynthetic performance (Baker, 2008).

There are four main competing forces when light quanta are absorbed by the Chl *a* (Krause and Weis,1991; Rohacek, 2002). It takes a certain amount of time for the Chl *a* molecule to return to its ground state after being excited by the incident light quanta. As a result, each of these four processes can be given a constant depending on the rate Chl *a* returns to its ground state. Rates of photochemical reaction (k_P), thermal deactivation (k_D), excitation energy transfer (k_T) and fluorescence (k_F) can be related to fluorescence emission (F). The quotient of the sum of the constants ($\Sigma\ k_I$) by k_F is directly proportional to F and can be related mathematically in equation 2.1. Absorbed light flux (I_a) is the perceived intensity of the incident light. It is directly proportional to F and therefore can also be incorporated into equation 2.1. The fluorescence yield (ΦF) is described as ratio of the fluorescence emission (F) compared to the intensity of the incident light (I_a) and can incorporated into equation 2.2.

2.1) $$F=I_a\ (k_F/\ \Sigma\ k_i)= I_a\ _X\ \ k_F/(\ k_P+\ k_D+\ k_T+\ k_F)$$

2.2) $$\Phi F=F/\ I_a= k_F/\ (k_P+\ k_D+\ k_T+\ k_F)$$

Equation 3 shows the relationship between photochemical yield (ΦP) and the rate constants. It is formed similarly to equation 2.2.

2.3) $$\Phi P= k_P/\ (k_P+\ k_D+\ k_T+\ k_F)$$

Fluorescence yield (ΦF) is very low when reaction centers are “open” (quinone pool is fully oxidized and able to accept electrons) and k_P is much greater than k_D, k_T and k_F. It is known that under low light and optimal temperatures (25^{o}C) in excess of 90% of absorbed light is used for photochemistry (Rohacek 2002). As a result, this situation is referred to as minimal

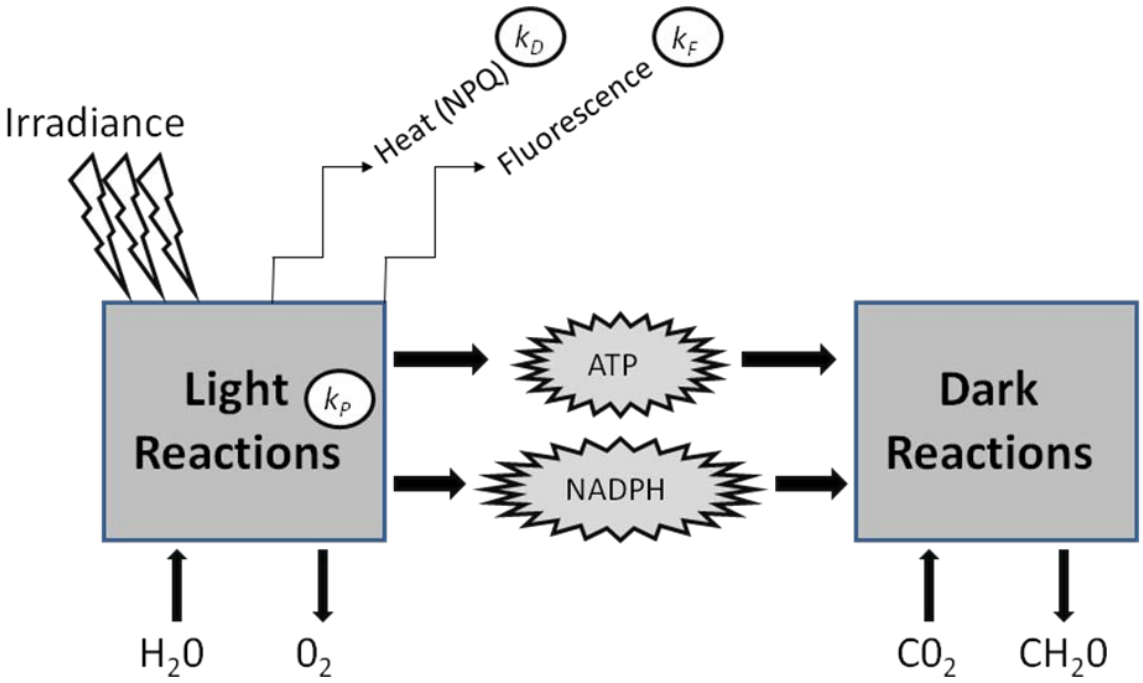

Fig. 2.3. Overview of reactants and products in photosynthesis. Also shown are the rate constants of the reactions k_D , k_P and k_F that compete for excitation energy from the sun's irradiance.

fluorescence yield (ΦF_O). Conversely, when the reaction center is "closed" (quinone pool is fully reduced), k_P is nearly equal to zero and the maximal fluorescence (ΦF_M) can be determined. ΦF_M refers to a situation where the reaction center is closed and all the rate constants are summed together. The value of k_P can be resolved when the difference between the fluorescent yields of both "open" and "closed" states is known. Therefore one can turn equation 2.3 into one that relates photochemical yield to fluorescent yield (equation 2.4).

2.4) $$\Phi P = (\Phi F_M - \Phi F_O)/ \Phi F_M = \boldsymbol{F_V/F_M}$$

Variable fluorescence yield (F_V) is the difference between maximal and minimal fluorescent yields (F_M-F_O). From equation 4 it is evident F_V/F_M is directly related to photochemical yield and can effectively gauge the photochemical efficiency of PSII. This ratio can be measured easily in a laboratory setting and imaging technology has facilitated the use of chlorophyll fluorescence as a method of determining the extent of photosynthetic stress caused by photoinhibition (Gray *et al.*, 2003; Baker and Rosenqvist, 2008).

2.4.2 Infra-red gas analysis

An infra-red gas analysis (IRGA) system is an invaluable tool in determining photosynthetic rate (Parsons *et al.*, 1997). The instrument provides *in vivo* photosynthetic rates by monitoring gas exchange in a sealed chamber. In this method, a sealed chamber (of a fixed volume) is placed over a photosynthetically active leaf (of a fixed area). The analyser can then determine the concentration of CO_2 in the chamber and monitor the evolution or disappearance of CO_2 over a time course. From the concentration values carbon assimilation rate can be expressed as amount of CO_2 assimilated per area and time (Farquhar *et al.*, 1980). This parameter (A) is a widely accepted and common measure of photosynthetic rate (Harbinson *et al.*, 1990; Seaton and Walker, 1990; Parsons *et al.*, 1997).

IRGAs also monitor humidity levels of the air in the chamber so water transpiration rate, stomatal conductance and water-use efficiency can also be calculated (Ireland *et al.*, 1989). Different experiments can also be created using varying levels of irradiance and intracellular CO_2 concentration which gives insight into maximal photosynthetic rates and photosynthetic/photorespiratory compensation points.

2.4.3 Light-response curves

Using photosynthetic modelling software, one can estimate other photosynthetic properties quickly and efficiently. The software uses the equations of Prioul and Chartier (1977) to estimate A_{max} (light saturated assimilation rate), Φ_a (apparent quantum efficiency), light compensation point, light saturation point and R_1 (dark respiration rate) from the shape of a modelled *A/Q* (irradiance) curve (Fig. 2.4). To construct an *A/Q* curve, the user records carbon assimilation rate over varying, and eventually, saturating irradiance levels. A_{max} is defined as the carbon assimilation rate (µmol CO_2 m^{-2} s^{-1}) at saturating irradiance at the light saturation point (µmol photons m^{-2} s^{-1}). Φ_a (µmol CO_2/µmol photons) is the slope of the initial section of the *A/Q* curve and is used to describe photosynthesis during a dark to light transition. The light compensation point (µmol photons m^{-2} s^{-1}) is the irradiance where the rate of carbon assimilation equals cellular respiration and R_1 (µmol CO_2 m^{-2} s^{-1}) is the rate of cellular respiration in the dark.

2.4.4 CO_2-repsonse curves

The equations of Olsson and Leverenz (1994) are used to estimate A_{max} (CO_2 saturated assimilation rate), CE (carboxylation efficiency), Resp (respiration in the light) and Γ (CO_2 compensation point), from the *A/Ci* curve (Fig 2.5). This curve is performed similarly to the *A/Q* curve except C_i is varied and irradiance is constant and saturating. Carboxylation efficiency (mol CO_2 m^{-2} s^{-1}) is defined as the slope of the initial curve while Resp (µmol CO_2 m^{-2} s^{-1}) is the Y-intercept of the line. Additionally, Γ (µmol CO_2 mol^{-1}) is found at the X-intercept of the modelled curve and is the internal leaf concentration needed to balance cellular respirations at saturating irradiance.

Harley and Sharkey (1991) have described equations to estimate $V_{c,\ max}$ (maximum carboxylation rate), J_{max} (electron transport rate) and TPU (triose phosphate utilization rate) also from the A/Ci curve. $V_{c,\ max}$ (µmol m-2 s^{-1}) can be estimated by equation 2.5. J_{max} (µmol m-2 s^{-1}) and TPU can be calculated by equations 2.6 and 2.7, respectively. These values combined with chlorophyll fluorescence provide the researcher with insight into photosynthetic of processes.

2.5) *Rubisco Activity=*$V_{c.max}$ x *Ci/[Ci+rubisco* K_{CO2}*(1+*O_2 *conc./rubisco* K_{O2}*)]*

2.6) *Apparent electron transport=eff. light conv.* x I_a */√[1+(eff. light conv.* x I_a */*J_{max}*)*^{2}*]*

2.7) *Regeneration rate of Pi= 3(TPU)+0.5* x V_o x O_2 *conc./Ci* x *spec. factor for rubisco*

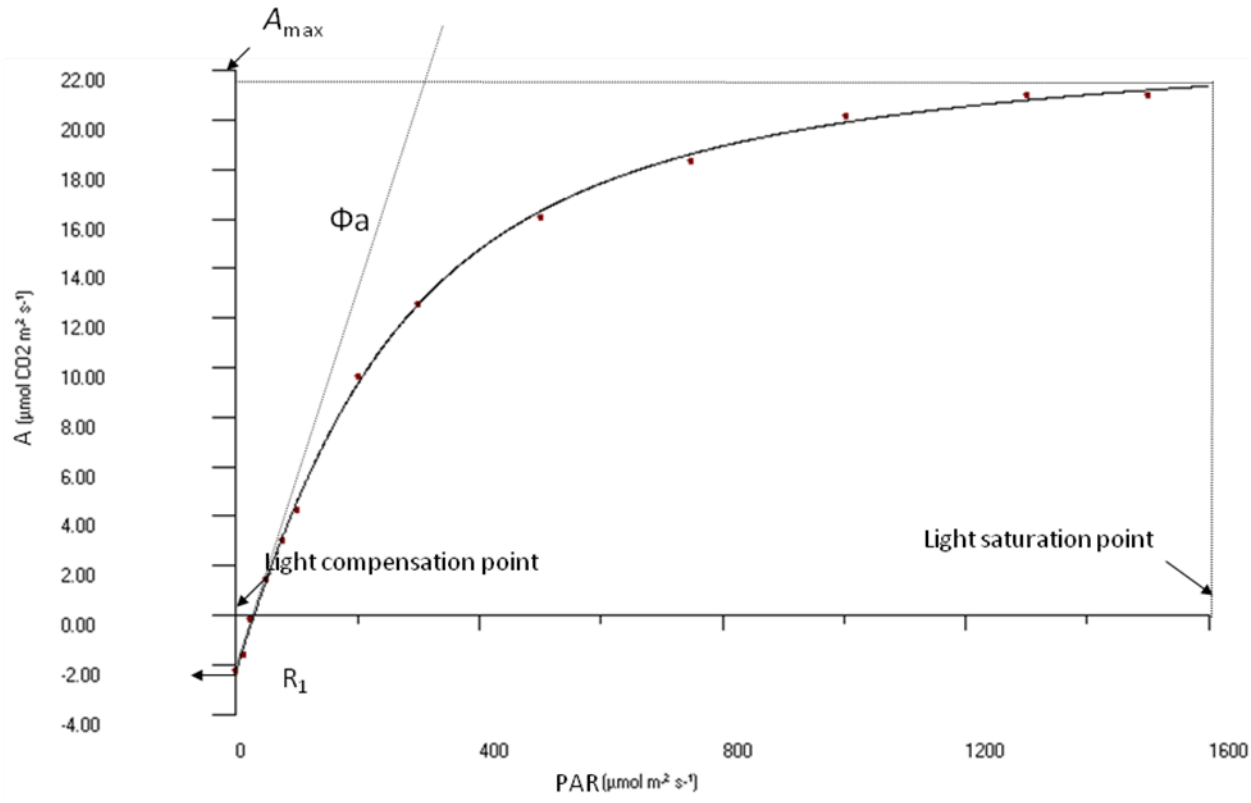

Fig. 2.4. Representation of A/Q(irradiance) curve. Also shown are the photosynthetic parameters : A_{max} (light saturated assimilation rate), Φ_a (apparent quantum efficiency), Light compensation point, Light Saturation point and R_1 (dark respiration rate) all calculated from the modeled curve. In this test, external CO_2 is constant and irradiance is increased stepwise from the dark until it reaches a saturating point (A_{max}).

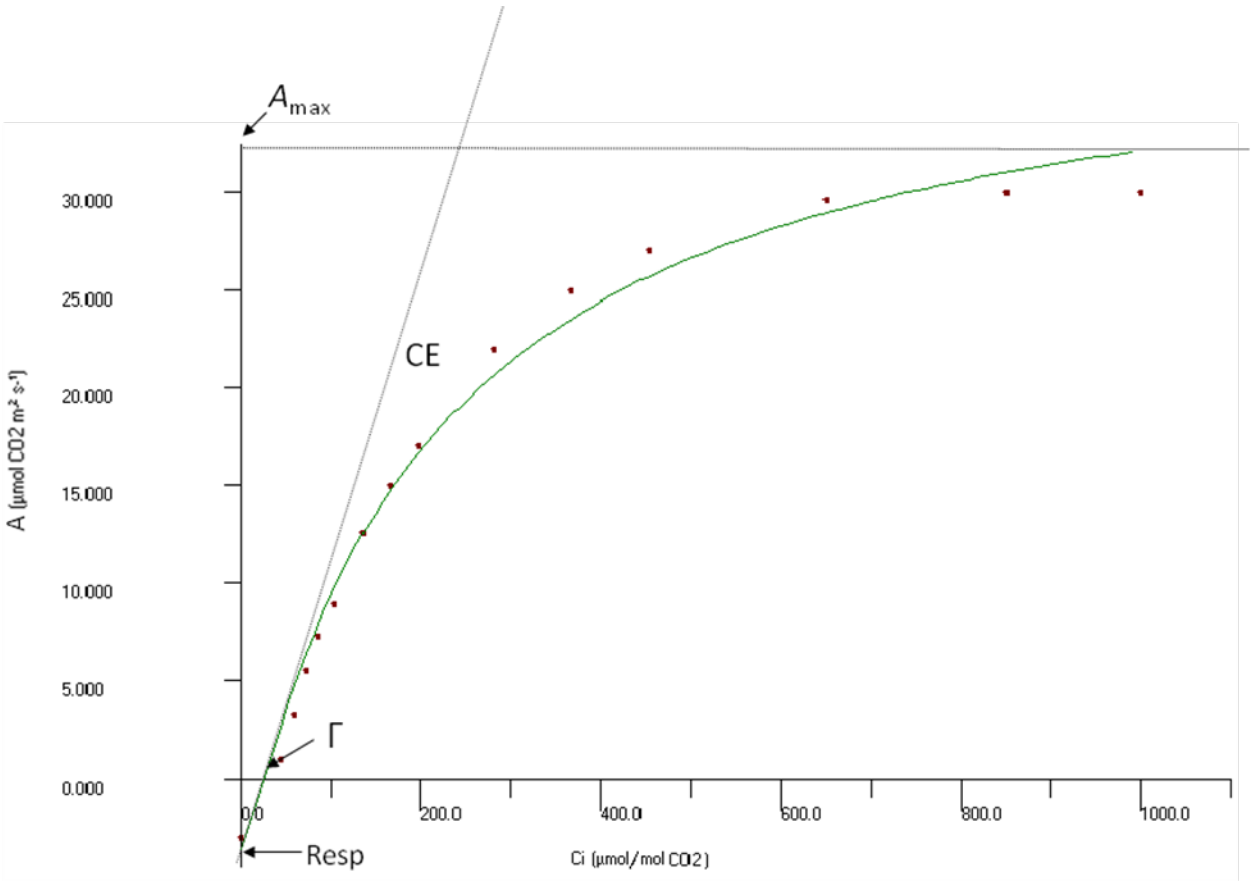

Fig. 2.5. Representation of A/Ci curve. Also shown are the photosynthetic parameters: A_{max} (CO_2 saturated assimilation rate), Γ (CO_2 compensation point), CE (carboxylation efficiency) and Resp (cellular respiration in the light), all calculated from the modelled curve. In this test, internal leaf CO_2 concentration is varied until saturating (A_{max}) while irradiance is constant and saturating.

2.4.5 Spectral Reflectance

Pigment composition is one of the most defining features of a plant. Chlorophyll is the initial acceptor of radiant energy and is integral to photosynthetic processes. It is therefore necessary to quantify chlorophyll content. Since chlorophyll absorbs and reflects light at defined wavelength it can be approximated by reflectance measurement parameters. The most popular chlorophyll index is Normalised Difference Vegetation Index (NDVI). It is based on the reflected amounts of a near infrared (740 nm) wavelength and very close visual (660 nm) wavelength of light (Gamon *et al*., 1999). Relative amounts not absorbed by the chlorophyll are reflected back and are measured. These figures can be placed in equation 2.8 and a unit less index number results. Numbers are usually close to but not over one.

2.8) $NDVI=(R_{740}-R_{660})/(R_{740}+R_{660})$

Photochemical reflective index (PRI) is another reflectance parameter based on light absorbance/reflectance of leaf pigments (Gamon *et al*., 1999). PRI is considered a good measure of xanthophyll induction. Xanthophylls, primarily zeaxanthin and antheraxanthin, are carotenoid leaf pigments that absorb excess light energy during photoinhibition to protect the plant and purposely lower photochemical efficiency (Demmig-Adams and Adams, 1996; Stylinski *et al.*, 2002). Like NDVI, PRI is an index based on reflected amounts of light at defined wavelength. PRI uses two different wavelengths, 530 nm and 570 nm, to quantify the amount of light absorbed based on how much is reflected. The light absorbed corresponds to the amount of zeaxanthin and antheraxanthin pigments currently present. PRI index calculation is shown in equation 2.9. PRI numbers are usually negative and become more positive as zeaxanthin and antheraxanthin are introduced.

2.9) $PRI=(R_{530}-R_{570})/(R_{530}+R_{570})$

2.5 Lignocellulosic biomass as fuel

Lignocellulosic biomass makes up the bulk of a plant's dry weight (Sun and Cheng, 2002). Cellulose and hemicellulose are glucose polymers and are major structural components of the plant cell wall overall plant biomass. They are polymerized by a variety of cellulose synthase enzymes. Among other biomass constituents are lignins. Lignins are long polymers of cinnamoyl-alcohols derived from phenylpropanoids (Vincent *et al.*, 1997; Baucher *et al.*, 1999). Enzymes that modify, store and polymerize phenylpropanoids are considered integral to the

lignin biosynthetic pathway.

Recent global energy concerns have spawned consideration of alternate fuels for energy purposes. Among alternative fuels is cellulosic ethanol which is made by anaerobically fermenting plant sugars into ethanol, an octane substitute (Sun and Cheng, 2002). Neither lignin nor hemicellulose can be fermented into ethanol and are antagonistic to the fermentation process. It has been demonstrated that cellulose and lignin contents are inversely proportional (Baucher *et al.*, 1999). The ideal wheat straw for fermentation would have high cellulose content and therefore low lignin content.

2.6 Market varieties of wheat and their uses

Wheat (*Triticum* spp.) is not only one of the most cultivated cereal crops in the world agriculturally, but also experimentally. It is popular as a C_3 photosynthesis model plant in cold stress studies mainly because it has both spring and winter-hardy varieties (Huner *et al.*, 1993). Previous studies have characterised cold-acclimated photosynthesis of wheat but few have focused on CO_2 growth or cultivar variation (Hurry *et al.*, 1995; Gray *et al.*, 1996). There are a wide choice of market varieties grown in western Canada, each with its own specific use and species (McCallum and DePauw, 2008). Within each market variety, cultivars are bred as an improvement over its predecessors but still conform to the standard of the final product. Table 1 displays the seven major market varieties grown in western Canada and distinguishing features.

Canada Western Red Spring (AC Barrie, McKenzie, Superb) is the most common of all wheat grown on the Prairies and is mostly used for all-purpose flour milling (McCallum and Depauw, 2008). Canada Western Amber Durum (Kyle and AC Avonlea) are ground into semolina which is used for pasta. Canada Prairie Spring Red (5700 PR and AC Crystal) is used for ethanol and animal feed while Canada Western Extra Strong (Glenlea) are used for specialty breads. The flour from Canada Western Soft White Spring Wheat (AC Andrew) is used for ethanol production and pastry flour. Canada Western Hard White Spring (Snowbird) and Canada Prairie Spring White (AC Vista) are both tailored for the Asian market and are used to make noodles (McCallum and Depauw, 2008).

Table 2.1: **Wheat cultivars utilized in this study (Canadian Wheat Board, 2006).** Values for "% seeded acres" are based on survey results specific to Saskatchewan 2006. DH, doubled haploid

Market Variety	Cultivar	% Seeded Acres of Market	Year Registered	Species	Ploidy	Parents	Uses	Growth Traits	Reference
Canada Western Red Spring	Superb	17.7	2001	*Triticum aestivum* L.	Hexa	Grandin*2/ AC Domain	All purpose flour/ white bread	High Yield	McCallum and DePauw 2008
	AC Barrie	16.5	1994			Neepawa/ Columbus/ /BW90		Yield/Rust Resistance	McCaig et al. 1996
	McKenzie	15.5	1997			DH Columbus/ Amidon		Yield/Rust Resistance	Graf et al. 2003
Canada Western Hard White Spring	Snowbird	96.8	2004	*Triticum aestivum* L.	Hexa	Poso48/RL 4137//AC Domain	Noodles	Yield/Disease Resistance	Humphries et al. 2007
Canada Prairie Spring White	AC Vista	87.9	1996	*Triticum aestivum* L.	Hexa	HY344/Lo sprout'S'// HY358*3/ BW553	Noodles	Yield/Sprout Resistance/ Disease Resistance	DePauw et al. 1998
Canada Western Amber Durum	AC Avonlea	39.0	1997	*Triticum turgidium* L	Tetra	8267-AD2A/dt6 12	Pasta	Yield/Protein	Clarke et al. 1998
	Kyle	24.3	1984			Wakooma/ DT322?? Wakooma/ DT320		Yield/Disease Resistance	Townley-Smith et al. 1987
Canada Western Extra Strong	Glenlea	58.2	1972	*Triticum aestivum* L.	Hexa	Pembina/Bage//CB100	Blended to add gluten strength	Yield/Rust Resistance	Evans et al. 1972
Canada Prairie Spring Red	AC Crystal	42.2	1996	*Triticum aestivum* L.	Hexa	HY377/L8474-D1	Feed/ethanol	Yield/Bunt Resistance	Fernandez et al. 1998
	5700 PR	36.1	2000			Pioneer 2369/ Probrand 711// AC Foremost		Yield/Rust Resistance	McCallum and DePauw 2008
Canada Western Soft White Spring	AC Andrew	100	2001	*Triticum aestivum* L.	Hexa	Dirkwin/SC8021V2// Treasure/Blanca	Pastry flour/ethanol	Yield/Disease Resistance	Sadasivaiah et al. 2004
Canada Western Red Winter	CDC Buteo	26.2	2001	*Triticum aestivum* L.	Hexa	S86-808/Abilene	Flat breads/ French Breads	Yield/Rust Resistance	McCallum and DePauw 2008
	CDC Clair	18.4	1995			Archer/Norstar			Fowler 1997
	CDC Raptor	17.7	2000			S86-808/Abilene			Fowler 2002
	CDC Falcon	6.8	1998			Norstar/Vona//Abilene			Fowler 1999

3.0 PHOTOSYNTHESIS IN THE FIELD

3.1 Introduction

Recent global energy concerns have prompted studies examining alternate fuels for energy purposes. One such fuel which has received much attention is cellulosic ethanol. This compound can be made by anaerobically by the fermentation of wheat straw, available as a by-product of grain production, into ethanol which can then serve as an octane substitute (Sun and Cheng, 2002). The main constituents of wheat straw are cellulose, hemicellulose and lignin. Together, these components are referred to as lignocellulosic biomass and comprise the bulk of a plants dry weight.

Through the reactions of photosynthesis, plants are able to convert sunlight into usable chemical energy by a direct reduction of CO_2 into triose phosphates by the enzyme Rubisco in the Calvin cycle. The assimilated CO_2 is then utilized for sucrose biosynthesis which in turn is used for growth and development. Thus, it is clear that photosynthetic performance and biomass accumulation are closely related (Ensminger *et al*., 2006)

However, the excess absorption of sunlight can lead to a phenomenon known as photoinhibition (Long *et al.*, 1994; Osmond and Grace, 1995; Takahashi and Murata, 2008). This occurs when high or even moderate amounts of light decrease the rates of photosynthetic activity often causing damage of the photosynthetic apparatus. Photoinhibition occurs on a daily basis for many photosynthetic organisms and limits yields of many crop species. The effects are exacerbated when their growth is limited by environmental factors such as extremes of temperature, light, drought and salinity (Takahashi and Murata, 2008). Susceptibility to photoinhibition varies among species and cultivars but is dependent on the ability of the plant to modulate photosynthetic reactions (Ensminger *et al*., 2006). An intricate balance must be maintained between photochemical processes and the utilization of their by-products (ATP and NADPH), primarily by the Calvin cycle for CO_2 assimilation (Huner *et al.*, 1993; Ensminger *et al.*, 2006).

Our goal in this study was to determine if there was any advantage to growing certain cultivars of wheat for their alternative uses, such as that of biofuel. This was accomplished by determining biomass accumulation, straw composition as well as characterizing photosynthesis and susceptibility to photoinhibition in several common cultivars of spring wheat grown in the

field over the 2007 and 2008 growing seasons in Saskatchewan.

3.2 Materials and methods

3.2.1 Plant material

Eleven spring wheat (*Triticum* spp.) cultivars comprising seven market varieties were selected for study based on percentage of seeded acres in Saskatchewan for the calendar year 2006 (Canadian Wheat Board, 2006; Table 2.1). These 11 cultivars were examined in the 2007 field experiments and based upon preliminary results four of these cultivars were chosen for further analyses in the 2008 field studies. Seeds were obtained from the Crop Development Centre at the University of Saskatchewan (Saskatoon SK).

3.2.2 Preliminary 2007 experiments.

As mentioned previously, all eleven spring varieties were planted during the growing season of 2007 at the Crop Science Field Laboratory. Starting at the fourth floret stage, F_V/F_M, PRI and NDVI measurements were made in triplicate using portable field equipment (refer to *3.2.6* and *3.2.7*). Measurements were made weekly until the cultivars were finished flowering (Table A1). Leaves were then harvested and subjected and 8 h photoinhibitory treatment as described in *3.2.8*. Two weeks later, NDVI, PRI, F_V/F_M, and measurements were performed on field wheat that was mature.

3.2.3 Field site

Two sets of field experiments were conducted from 2007 to 2008. Spring wheat lines were grown on fallowed land at the Seed Farm, University of Saskatchewan (Saskatoon SK) on a Dark Brown Chernozem clay loam soil type. Each plot consisted of a single row that was 1.3 m long spaced 0.3 m apart. Plots were sown on May 1 and 3, in 2007 and 2008, respectively. The seeding rate was approximately 100 seeds per row at a seeding depth of 2 cm. Fertilizer (11-51-0) was drilled in with the seed at a rate of 7 kg ha^{-1} of N and 29 kg ha^{-1} of P. Weed control was achieved using recommended rates of the herbicides Buctril-M (Aventis CropScience Canada Co., Regina, SK; active ingredients bromoxynil and MCPA) tank-mixed with Horizon (Syngenta Crop Protection Canada, Inc., Guelph, ON; active ingredient clodinafop-propargyl). A randomized complete block design with four replications was used in both years. Data was

collected from random positions in each of the four replications over the growing season and averaged. For biomass determinations whole plants were removed from the field in August 2007, hand picked to ensure root injury was minimal. Samples of wheat straw were collected in September 2007 at the end of the growing season after harvest.

3.2.4 Meteorological data

Temperature, rainfall and solar radiation data from April through October in 2007 and 2008 were collected within 6 km of the trial site at the Kernen Crop Research Farm weather station, University of Saskatchewan (Saskatoon SK).

3.2.5 Measurements of CO_2 exchange

In situ CO_2 exchange rates were measured under field conditions on wheat leaves using a portable open circuit steady-state gas-exchange system incorporating an infrared gas analyzer (model LI-6400, Li-Cor, Lincoln, NB). Measurements were made on the mid-portion of flag--leaves and corrected for leaf area in the sample chamber. The cuvette measuring temperature was set to 20°C. Simultaneous measurements of CO_2 to H_2O vapour flux, air (T_{air}) and leaf (T_{leaf}) temperature allowed for the calculation of leaf carbon assimilation (A), stomatal conductance to water (g_s), transpiration rate (E), intercellular CO_2 partial pressure (C_i) and leaf to air vapour pressure difference calculated from T_{leaf} (*vpdL*).

Light-response curves (*A/Q*) were obtained using the range of 0-1500 µmol m^{-2} s^{-1} PPFD. Irradiance was provided from a red-blue LED light source (LI-6400-02B, Li-Cor) attached to the sensor head. The PPFD was increased in 12 steps and the sample was allowed to acclimate to the PPFD until stable values had been attained prior to acquiring data and moving to the next irradiance value. Ambient CO_2 partial pressure (C_a) was maintained at a concentration of 400 µmol mol^{-1} using a CO_2 mixer/injector (LI-6400-01, Li-Cor). This resulted in intracellular CO_2 concentrations (C_i) ranging from 206-440 µmol mol^{-1} over the course of the experiment. Humidity of incoming air was controlled at 0.90-2.5 kPa *vpdL* based on T_{leaf} which did not exceed 29°C at any time during the experiment, resulting in humidity values of 57-82%.

A/C_i curves were constructed at a saturating PPFD of 1300 µmol m^{-2} s^{-1}. Leaves were exposed to 400 µmol mol^{-1} C_a until stable. C_a was decreased stepwise to a lower concentration of 50 µmol mol^{-1} and then increased stepwise to an upper concentration of 1200 µmol mol^{-1}.

This resulted in C_i values ranging from to 48 to 872 µmol mol^{-1}. Humidity of incoming air was controlled at 1.9-4.4 kPa *vpdL* based on T_{leaf} which did not exceed 33°C at any time during the experiment, resulting in humidity values of 58-89%.

A/Q and A/C_i curves were repeated in triplicate and each curve was modeled using analysis software (Photosyn Assistant, Ver. 1.2; Dundee Scientific, UK) for the determination of several photosynthetic parameters (Parsons *et al*., 1997). Parameters calculated are described in *2.4.4*. Intrinsic water use efficiency (WUE) was calculated as *A*/*E*, and was determined at a PPFD of 1500 µmol m^{-2} s^{-1} and ambient CO_2, as were values of g_s and *E*.

3.2.6 Spectral Reflectance

Reflectance measurements were obtained in the field on flag leaves using a hand-held device designed to measure reflectance at fixed wavelength. The Normalized Difference Vegetative Index (NDVI) was determined using a PlantPen NDVI 300 while photochemical reflective index (PRI) was determined by a PlantPen PRI 200 (Photon Systems Instruments, Czech Republic). NDVI values were calculated according to NDVI = $(R_{740}-R_{660})/(R_{740}+R_{660})$. The NDVI is a unit-less index and was used as an estimate of Chl content and leaf biomass (primary productivity). Usually, a healthy, growing plant will have an NDVI number around 0.8 and will decrease with less chlorophyll content. PRI values were calculated by PRI = $(R_{530}-R_{570})/(R_{530}+R_{570})$. PRI numbers are usually negative and become more positive as zeaxanthin and antheraxanthin accumulate and violaxanthin decreases. An unstressed plant will have PRI around -0.5 while a stressed plant will increase to nearly 0.5.

3.2.7 Chlorophyll fluorescence

Chlorophyll *a* fluorescence measurements in the field were performed on flag leaves with a hand-held pocket fluorometer (FluorPen FP100; Photon Systems Instruments, Czech Republic).The leaves were dark-adapted for 15 min before measurement. The maximum quantum photochemical) efficiency of PSII was calculated as $F_V/F_M = (F_M-F_O)/F_M$, where F_O and F_M represent the minimal and maximal fluorescence yield in the dark-adapted states, respectively. For photoinhibition experiments (see section 3.2.8 below), F_V/F_M was determined using a Chl fluorescence imaging apparatus as described previously (Gray *et al.*, 2003; Baerr *et al.*, 2005).

3.2.8 Low-temperature photoinhibition

Photoinhibition of photosynthesis was induced at leaf temperatures between 5 and 7°C for a total of 8 h under ambient air conditions. Flag leaves were harvested from each cultivar and brought into a laboratory cold room. Leaves were placed adaxial side up on moist paper towels and exposed to an irradiance of 1450 µmol m^{-2} s^{-1} PPFD essentially as described by Gray *et al*. (1996). Susceptibility to photoinhibition was quantified by monitoring changes in F_V/F_M as a function of exposure time. Dark controls and long-term photoinhibition experiments were performed for validation purposes (data not shown).

3.2.9 Pigment extraction and determination

Leaves used for pigment analyses were harvested and their fresh weight (FW) determined followed by flash freezing in liquid nitrogen. Leaf material was stored at -80°C until pigment extraction.

Pigments were extracted in a microfuge tube by homogenization in 0.5 mg FW mL^{-1} 100% (v/v) HPLC-grade acetone (OmniSolv; BDH Inc., Toronto, Ontario, Canada), with 0.3 mg mL^{-1} $CaCO_3$, at 4°C in dim light using 1 mm glass beads and an agitation apparatus (Mini-Bead Beater-1; BioSpec Inc., Bartlesville, OK). The tube was shaken for 5 min at the maximum speed, followed by centrifugation at 6,000 *xg* for 8 min at 4°C. The supernatant was passed through a 13 mm, 0.2 µm PVDF -syringe filter (Pall Life Sciences, East Hills, NY) into sample vials prior to storage under nitrogen at -80°C in the dark until HPLC analysis.

Analysis of leaf acetone extracts was performed using a HPLC system (System Gold; Beckman-Coulter Inc., Fullerton, CA) described earlier (Baerr *et al.,* 2005). Pigments were separated by reverse-phase HPLC analysis with a C18 column (Thermo ODS Hypersil; 4.6 mm x 60 mm, 3 µ pore size; Thermo Scientific, Waltham, MA) protected by a C18 TSK guard column (6.0 mm x 40 mm, 7 µ pore size; Beckman-Coulter). The protocol of Buch *et al.* (1994) was used with minor modifications. The mobile solvent phase consisted of 60% (v/v) acetone in aqueous buffer (1 mM HEPES, pH 7.0). Elution was performed using a gradient program which consisted of a 15 min linear gradient to 72.5% (v/v) acetone; followed by a 5 min linear gradient to 75% (v/v) acetone; followed by a 5 min linear gradient to 80% (v/v) acetone; followed by 30 min linear gradient to 98% (v/v) acetone which continued isocratically for 10 min. The total run

time was 55 min at room temperature with a flow rate of 0.4 mL min^{-1}.

Pigment peaks were identified by comparing retention times and spectra relative to those of known standards. Pigments were detected at 445 nm and peak areas were integrated using System Gold software (32 Karat, version 5.0) to allow for the calculation of concentrations, expressed on a total Chl basis. Purified standards of Chl *a*, Chl *b*, β-carotene and lutein were purchased from Sigma-Aldrich (Oakville, ON). Standards of neoxanthin, violaxanthin, antheraxanthin and zeaxanthin were purified from photoinhibited spinach leaves using a TLC method (Diaz *et al.*, 1990). Concentration and identification of standards were performed using a Bio-Rad SmartSpec Plus spectrophotometer (Bio-Rad, Philadelphia, PA). The equations of Holm (1954) were used to quantify standards of Chl *a* and Chl *b* while the equations of Bernhard and Grosjean (1995) were used to quantify standards of neoxanthin, violaxanthin, antheraxanthin, zeaxanthin, lutein and β-carotene.

The epoxidation state (EPS) of the samples were estimated according to Thayer and Bjorkman (1992) as EPS = (V+0.5A)/ (V+A+Z), where V, A, and Z correspond to the concentrations of the xanthophyll carotenoids violaxanthin, antheraxanthin, and zeaxanthin, respectively. Xanthophyll pool size was calculated as the sum of violaxanthin, antheraxanthin, and zeaxanthin (V+A+Z).

3.2.10 Biomass accumulation and composition

Field grown plants were harvested, separated into roots and shoots and fresh weight (FW) was determined. They were then placed into a drying oven (Labco, Lucknow, India) for a minimum of 48 h at 90°C or until constant weight was obtained for the determination of dry weight (DW). Wheat straw composition was determined using an Ankom Model 200 Fiber Analyzer (Ankom Technology, Macedon, NY). Standard fiber detergent analysis methods (Van Soest and Wine, 1967; Poore *et al.*, 1991) were used as described by the manufacturer.

3.3 Results

3.3.1 Preliminary results of 2007 growing year

Upon inspection of the data, there was very little difference in the measured parameters between cultivars and many were indistinguishable from one another (Table A1). This could be due to the high variance of developing in a field environment. Photochemical efficiency varied

throughout the assortment of spring wheat cultivars. Additionally, xanthophyll pigment induction (PRI) was not altered by varying solar irradiance or photochemical efficiency.

When field leaves were placed under photoinhibitory conditions, differences were seen between cultivars (Fig A1). Most cultivars had decreased photochemical efficiencies of 5-10% over the first two h of treatment. Many of the cultivars also displayed a quick decrease in photochemical efficiency over the first four h then a gradual decrease over the remainder. There were some exceptions, however. The amber durum cultivar, Kyle, had an immediate decrease in photochemical efficiency of 30% over the first four h only, then a slight recovery for the remainder of the treatment. Glenlea, an extra strong cultivar, had the best photoinhibitory tolerance after 4 h only to severely decrease its tolerance for the remainder of photoinhibition (Figure A1).

3.3.2 Cultivar selection

For the first field experiment in 2007, 11 spring wheat cultivars comprising 7 market varieties were selected for study based on percentage of seeded acres in Saskatchewan for the calendar year 2006 (Table 2.1) as reported in the Canadian Wheat Board Variety Survey (2006).

Based upon the data obtained during the 2007 field experiments, 4 of the 11 cultivars examined were chosen for further analyses in the 2008 field studies. These included a Western Red Spring (McKenzie), a Western Amber Durum (Kyle), a Western Soft White Spring (AC Andrew) and a Western Hard White Spring (Snowbird). These particular cultivars were chosen primarily based on their tolerances to photoinhibition, cellulose contents and popularity among wheat growers. McKenzie was chosen due to its strong photoinhibitory resistance, high cellulose content and its popularity among wheat growers. Kyle is also popular among durum wheat growers and has low cellulose content and aberrant photoinhibitory characteristics in the field. AC Andrew also has great photoinhibitory tolerance and high biomass. Snowbird was chosen for further study because of its high cellulose content but poor photoinhibitory resistance in the field.

3.3.3 Meteorological data

During the 2007 and 2008 growing seasons seed was sown on May 1 and 3, respectively. The leaves were sampled for photosynthetic studies on July 4 and 10 in 2007 and 2008 respectively. Plants were harvested on August 20 in 2007 for compositional and biomass

analyses. No differences were observed in the daily average incoming solar irradiation between 2007 and 2008 (Fig A2). However, the mean rainfall decreased in 2008 (193 mm) in comparison to 2007 (297 mm; Fig A2). During both growing seasons the coldest month was May with average minimum temperatures of 4.2°C in 2007 and 2.3°C in 2008. In 2007, the maximum average temperature in the warmest month (July) was 27.5°C, while in 2008; the warmest month (August) presented a maximum average temperature of 25.3°C.

3.3.4 Photosynthesis and productivity

Non-destructive approaches for monitoring photosynthetic function, which include spectral reflectance indices (SRI) and chlorophyll fluorescence, are particularly attractive as they can be used at the level of the single leaf as well as on larger scales. Chlorophyll *a* fluorescence parameters provide an efficient and non-invasive tool by which to investigate photosynthetic processes as well as to detect environmental stress in the photosynthetic apparatus (Krause and Weis 1991). A useful measurement to quantify the latter is the maximal quantum yield of PSII photochemistry or the F_V/F_M ratio (Lu *et al.*, 2001; Baker and Rosenqvist, 2004). This ratio was used as an estimate of the photochemical efficiency of photosynthesis in these experiments. During plant stress, F_V/F_M will drop indicating a decrease in photochemical efficiency. This ratio can be measured easily in a field setting and is generally accepted as an index of plant health. In general, values exhibited minimal fluctuation among cultivars during the 2007 growing season (Table 3.1). The cultivars AC Barrie (0.73 ± 0.02) and Kyle (0.72 ± 0.06) showed the lowest values while AC Vista (0.78 ± 0.01) and 5700 PR (0.78 ± 0.03) demonstrated the highest values (Table 3.1).

One of the most widely used SRI is the Normalized Difference Vegetation Index (NDVI), an index that was developed to assess productivity of plants. NDVI is calculated as a normalized difference between the reflectances of two biologically meaningful bands of the electromagnetic spectrum. It relates the difference between near infrared (NIR) reflectance and red wavelength (VIS) reflectance with the reflectance of both wavelength. NDVI separates green vegetation from other vegetation by the absorption of red light by chlorophyll. These same leaves reflect the near-infrared wavelength due to scattering caused by internal leaf structure (Tucker, 1979; Wiegand *et al.*, 1991). The NDVI was determined in 2007 field samples and values ranged from 0.69 ± 0.02 in Kyle to 0.74 ± 0.01 in the cultivar 5700 PR (Table 3.1).

Table 3.1. Fluorescence (F_V/F_M) and reflectance (NDVI) parameters of wheat cultivars utilized in field experiments conducted in 2007 and 2008. Values were determined on flag leaf in the field using a portable fluorometer and reflectometer. Values represent means ± SD, (n = 3).

Market Variety	Cultivar	F_V/F_M	NDVI
2007 Growing Season			
Canada Western Red Spring	AC Barrie	0.73 ± 0.02	0.73 ± 0.01
	McKenzie Superb	0.76 ± 0.01	0.73 ± 0.01
		0.77 ± 0.01	0.73 ± 0.01
Canada Western Amber Durum	AC Avonlea	0.76 ± 0.02	0.72 ± 0.01
	Kyle	0.72 ± 0.06	0.69 ± 0.02
Canada Prairie Spring Red	AC Crystal	0.75 ± 0.02	0.73 ± 0.01
	5700 PR	0.78 ± 0.03	0.74 ± 0.01
Canada Western Soft White Spring	AC Andrew	0.75 ± 0.04	0.72 ± 0.01
Canada Western Extra Strong	Glenlea	0.76 ± 0.02	0.73 ± 0.02
Canada Western Hard White Spring	Snowbird	0.77 ± 0.02	0.70 ± 0.01
Canada Prairie Spring White	AC Vista	0.78 ± 0.01	0.72 ± 0.02
2008 Growing Season			
Canada Western Red Spring	McKenzie	0.80 ± 0.01	0.68 ± 0.01
Canada Western Amber Durum	Kyle	0.78 ± 0.01	0.64 ± 0.03
Canada Western Soft White Spring	AC Andrew	0.79 ± 0.01	0.68 ± 0.03
Canada Western Hard White Spring	Snowbird	0.80 ± 0.01	0.67 ± 0.03

During the 2008 growing season the 4 cultivars examined presented F_V/F_M values of 0.78 ± 0.01 to 0.80 ± 0.01 (Table 3.1). Values of NVDI were also relatively consistent among cultivars ranging from 0.64 ± 0.03 to 0.68 ± 0.01 (Table 3.1). The wheat cultivar Kyle presented the lowest values for each of these parameters (Table 3.1). NDVI responds to changes in biomass and chlorophyll content, and hence serves as a useful measure or primary productivity. High NDVI values therefore indicate high leaf biomass (Prasad *et al.*, 2009). In fact, NDVI has been proposed as a means of estimating biomass and photosynthesis (or yield) in wheat and other cereals (Aparicio *et al.*, 2000; Prasad *et al.*, 2009).

Rates of photosynthesis were also determined in the field during 2008 using CO_2 gas exchange. Light- (*A/Q*) and CO_2-response curves (A/C_i) were constructed for each of the cultivars (Figure A3) and these data were modeled and the photosynthetic parameters obtained are indicated in Table 3.2. *A/Q* curves were determined at ambient CO_2 concentrations of 400 µmol mol^{-1}, while A/C_i curves were measured at a saturating irradiance of 1300 µmol m^{-2} s^{-1}. All measurements were expressed on a leaf area basis. When examined for response to irradiance, the McKenzie cultivar demonstrated the highest values of A_{max} and Φ_a (Table 3.2). Snowbird exhibited the lowest Φ_a which was also reflected in its elevated light-compensation and saturation points. When the cultivars were examined in response to fluctuations of internal leaf CO_2 concentrations (*Ci*) Snowbird demonstrated a 19-22% lower A_{max} and elevated Γ (CO_2 compensation point) (Table 3.4). Carboxylation efficiency was 2.1- to 2.5-fold greater in McKenzie which also had the highest respiration and *WUE* values, as a result of lower *E* (Table 3.4). These data suggest that McKenzie is photosynthetically a superior cultivar while Snowbird may be less responsive to changing irradiance and CO_2 conditions.

3.3.5 Plant biomass

At the end of the 2007 growing season plants were harvested and biomass approximated by plant DW. These data are presented in Fig. 3.1A. The cultivars AC Avonlea, Kyle and Glenlea exhibited the greatest dry matter accumulation, followed by Superb and AC Vista (Fig. 3.1A). Overall, minimal differences were observed among the cultivars (Fig. 3.1A). Root to shoot ratios are presented in Fig. 3.1B and approximate carbon partitioning. Values were relatively consistent among the cultivars with Kyle, 5700 PR and Glenlea demonstrating greater partition to the root system (Fig. 3.1B).

Table 3.2. Photosynthetic parameters derived from modeled light- (*A/Q*) and CO_2-response (*A/C*$_i$) curves for wheat cultivars utilized in field experiments conducted in 2008. Values were determined on flag leaf in the field using a portable IRGA. Values represent means ± SD, (*n*=3).

Photosynthetic Parameter	McKenzie	Kyle	AC Andrew	Snowbird
A_{max} (µmol CO_2 m^{-2} s^{-1})[a]	40.30 ± 0.92	32.27 ± 1.10	34.60 ± 1.08	31.27 ± 1.23
Φ_a CO_2 (µmol CO_2/µmol photons)[a]	0.424 ± 0.019	0.346 ± 0.097	0.371 ± 0.022	0.245 ± 0.040
Light compensation point (µmol m^{-2} s^{-1})[a]	7.96 ± 0.80	7.71 ± 1.87	8.80 ± 2.61	9.03 ± 0.09
Light saturation point (µmol m^{-2} s^{-1})[a]	103.00 ± 2.65	105.77 ± 27.29	102.33 ± 6.03	138.67 ± 15.50
R_1 (µmol CO_2 m^{-2} s^{-1})[a]	-3.38 ± 0.48	-2.56 ± 0.31	-3.29 ± 1.15	-2.21 ± 0.37
A_{max} (µmol CO_2 m^{-2} s^{-1})[b]	99.20 ± 5.83	98.13 ± 8.24	94.50 ± 8.01	76.53 ± 2.01
CE (µmol CO_2 m^{-2} s^{-1})[b]	1.12 ± 0.50	0.51 ± 0.14	0.44 ± 0.09	0.54 ± 0.01
Resp (µmol CO_2 m^{-2} s^{-1})[b]	-32.90 ± 8.71	-24.93 ± 8.85	-19.63 ± 0.91	-24.62 ± 0.81
Γ (µmol CO_2 mol^{-1})[b]	45.5 ± 4.84	63.9 ± 8.98	57.3 ± 12.0	66.3 ± 3.75
$V_{c,max}$ (µmol m-2 s-1)[b]	123.1 ± 1.0	70.0 ± 8.1	83.1 ± 7.0	62.2 ± 0.32
J_{max} (µmol m-2 s-1)[b]	457.2 ± 98.8	330.3 ± 65.9	343.3 ± 2.1	235.7 ± 6.5
TPU (µmol m-2 s-1)[b]	19.5 ± 2.05	17.37 ± 0.64	20.5 ± 0.6	14.5 ± 0.45
Transpiration rate (mmol H_2O m^{-2} s^{-1})[c]	5.16 ± 0.10	7.34 ± 1.16	7.59 ± 2.10	7.55 ± 0.71
Stomatal conductance (mol m^{-2} s^{-1})[c]	0.313 ± 0.003	0.304 ± 0.005	0.323 ± 0.016	0.305 ± 0.061
Intrinsic water use efficiency (µmol CO_2 mmol H_2O^{-1})[c]	6.69 ± 0.18	3.98 ± 0.41	4.19 ± 1.44	3.65 ± 0.24

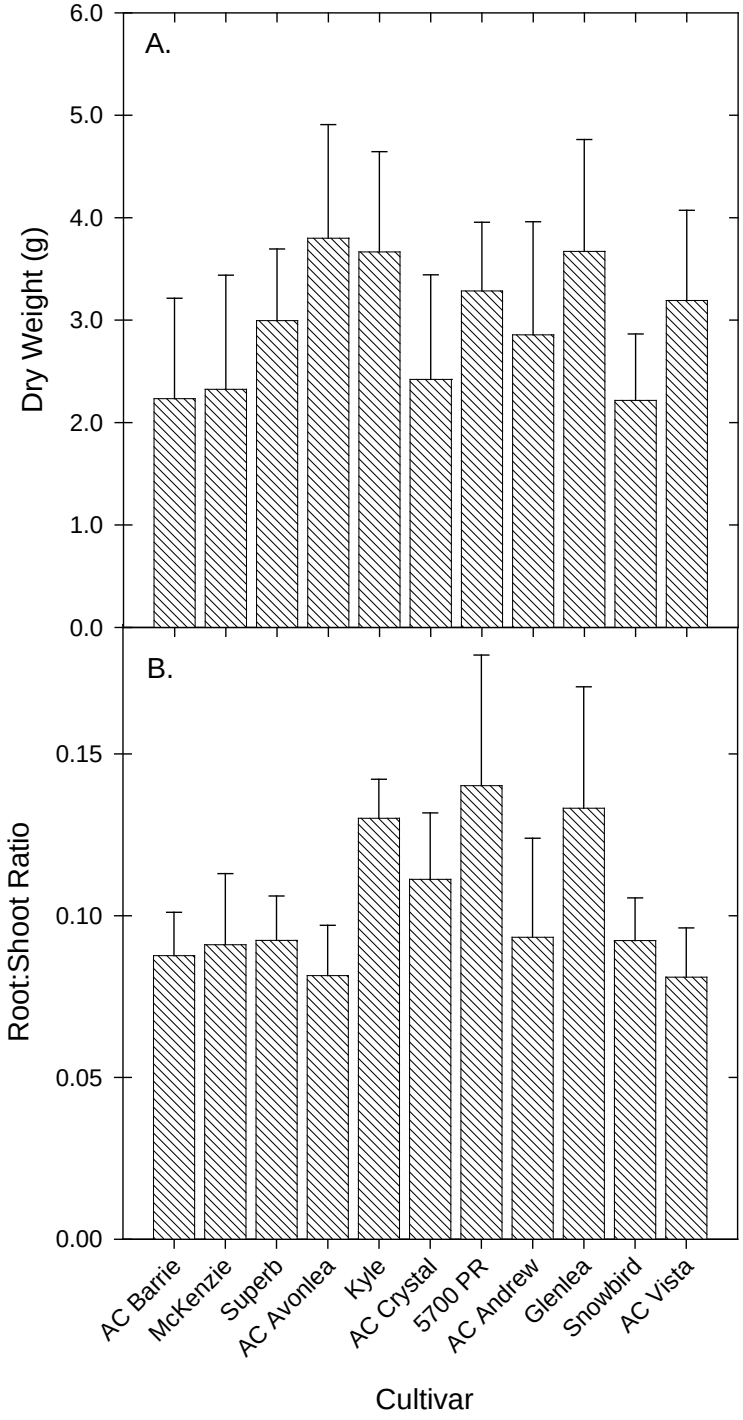

Fig. 3.1. Whole plant biomass accumulation as estimated by dry weight (A) and root:shoot ratios (B) in various cultivars of wheat grown in the field experiments conducted in the calendar year 2007. Values represent the means of individual whole plants ± SD, *n* = 6.

The composition of the wheat straw after combining in late August was also determined and is presented in Table 3.3. This procedure separates material into ash, lignin, cellulose and hemicellulose fractions. Cellulose and hemicellulose are sugar polymers and major structural components of the plant cell wall. Lignins are long polymers of cinnamoyl-alcohols derived from phenylpropanoids and usually associate with plant secondary cell walls (Baucher *et al*., 1999). Lignin content was 7.4 ± 0.1% in the cultivars AC Avonlea and 5700 PR, reaching up to 12.5 ±.0.1% in Kyle (Table 3.3). Cellulose content was 33.1 ± 0.6% in Kyle to 40.7 ± 0.1% in McKenzie while hemicellulose values ranged from 17.6 ± 0.3% in Glenlea to 23.6 ± 0.8% in AC Andrew (Table 3.3).

3.3.6 Susceptibility to photoinhibition

Exposure of leaves grown during 2008 to photoinhibition at low temperature resulted in a 49 to 53% decrease in normalized F_V/F_M values over 8 h compared to starting values (Fig. 3.2; Table 3.1). Minimal differences were present at 1 h but separation between cultivars became evident after 2 h which was maintained at the 4 h point. McKenzie was 11 and 12% more tolerant than Kyle at these points respectively (Fig. 3.2), with AC Andrew and Snowbird demonstrating intermediary values (Fig. 3.2). No difference between the cultivars was visible after 8 h (Fig. 3.2).

Plants utilize several mechanisms to alleviate the damage caused by absorbing more light than can be used for CO_2 fixation. A universal photoprotective process is the non-photochemical quenching (NPQ) of excess excitation energy in the light-harvesting antenna pigment bed of PSII (Malkin and Niyogi, 1999). While NPQ generation is a complicated process, the operation of the xanthophyll plays a major role. This cycle involves the de-epoxidation of a carotenoid pigment, violaxanthin into antheraxanthin and zeaxanthin (Demmig-Adams, 1992; Holt *et al.*, 2005).

The carotenoid levels were investigated both pre- and post-photoinhibition. Xanthophyll concentrations were normalized to chlorophyll as chlorophyll abundance varied little between samples (data not shown). In general, minimal differences were observed in β-carotene, lutein and neoxanthin between cultivars or as a result of photoinhibitory treatment (Table 3.4). Prior to photoinhibition, AC Andrew had the lowest amount of β-carotene (40 to 53% over the other cultivars) while Snowbird contained greater amounts of lutein compared to the other cultivars (1.6 to 1.8-fold; Table 3.4). Post-photoinhibition AC Andrew contained lower amounts of β-carotene (41 to 50%) and neoxanthin (39 to 56%; Table 3.4). While the pool size of xanthophyll

Table 3.3. Composition of wheat straw from cultivars utilized in field experiments conducted in 2007. A fiber detergent analyser was used on flag leaves. Values represent means ± SD, (*n* = 2). *NPE, non-polar extract.

Market Variety	Cultivar	% of FW				
		Ash	Lignin	Cellulose	Hemicellulose	NPE*
Western Red Spring	AC Barrie	4.6 ± 0.1	10.4 ± 0.1	38.8 ± 0.6	19.7 ± 0.1	26.4 ± 0.8
	McKenzie	4.6 ± 0.0	7.8 ± 0.0	40.7 ± 0.1	21.4 ± 0.5	25.5 ± 0.6
	Superb	3.8 ± 0.2	8.4 ± 0.2	39.3 ± 0.9	22.0 ± 0.0	26.6 ± 0.2
Western Amber Durum	AC Avonlea	2.8 ± 0.0	7.4 ± 0.0	38.7 ± 0.1	23.4 ± 0.3	27.7 ± 0.4
	Kyle	2.8 ± 0.1	12.5 ± 0.1	33.1 ± 0.6	19.1 ± 0.0	32.6 ± 1.2
Prairie Spring Red	AC Crystal	4.0 ± 0.2	12.2 ± 0.2	34.7 ± 0.1	23.5 ± 0.7	25.6 ± 1.1
	5700 PR	3.9 ± 0.0	7.4 ± 0.0	39.0 ± 0.1	22.5 ± 0.3	27.2 ± 0.1
Western Soft White Spring	AC Andrew	3.3 ± 0.2	7.8 ± 0.1	39.2 ± 0.6	23.6 ± 0.8	26.0 ± 0.7
Western Extra Strong	Glenlea	3.5 ± 0.0	8.1 ± 0.0	36.3 ± 0.5	17.6 ± 0.3	34.4 ± 0.9
Western Hard White Spring	Snowbird	5.0 ± 0.0	9.7 ± 0.0	39.3 ± 0.2	20.8 ± 0.2	25.2 ± 0.5
Prairie Spring White	AC Vista	3.3 ± 0.1	13.1 ± 0.1	35.6 ± 0.2	22.7 ± 0.7	25.2 ± 1.7

Table 3.4. Photosynthetic pigment content of wheat cultivars grown in the field during 2008 and utilized for photoinhibition studies. HPLC analysis was performed on flag leaf. Values represent the means ± SD, n = 3 *nd, not-detected.

Cultivar	β-C	L	N	V	A	Z	V+A+Z	EPS
	(mmol mol^{-1} Chl a+b)							
Pre-Photoinhibition								
McKenzie	84.6 ± 6.0	82.0 ± 11.4	21.0 ± 1.6	68.1 ± 6.3	3.1 ± 0.3	nd*	71.2 ± 7.3	0.98 ± 0.04
Kyle	66.8 ± 6.1	92.0 ± 4.7	24.6 ± 1.9	72.7 ± 5.6	3.1 ± 0.3	0.8 ± 0.8	76.7 ± 10.8	0.97 ± 0.06
AC Andrew	39.7 ± 2.1	93.3 ± 5.7	22.2 ± 1.8	53.6 ± 3.8	3.6 ± 0.4	0.9 ± 0.6	58.1 ± 11.2	0.95 ± 0.02
Snowbird	68.1 ± 7.1	146.4 ± 16.7	25.4 ± 1.5	72.1 ± 5.3	2.7 ± 0.2	nd	74.8 ± 13.8	0.98 ± 0.05
Post-Photoinhibition (8h)								
McKenzie	64.8 ± 6.0	99.0 ± 10.2	18.2 ± 1.7	nd	11.7 ± 0.9	63.5 ± 4.5	75.2 ± 6.0	0.08 ± 0.05
Kyle	59.2 ± 3.8	103.8 ± 12.9	25.0 ± 3.3	nd	12.3 ± 1.4	68.8 ± 4.7	81.2 ± 6.7	0.08 ± 0.03
AC Andrew	35.2 ± 2.5	105.0 ± 12.8	11.2 ± 1.0	nd	15.9 ± 1.6	50.6 ± 2.6	66.5 ± 4.7	0.12 ± 0.03
Snowbird	70.0 ± 5.1	102.5 ± 5.4	24.2 ± 2.2	nd	13.0 ± 0.7	63.5 ± 2.9	76.5 ± 4.0	0.08 ± 0.04

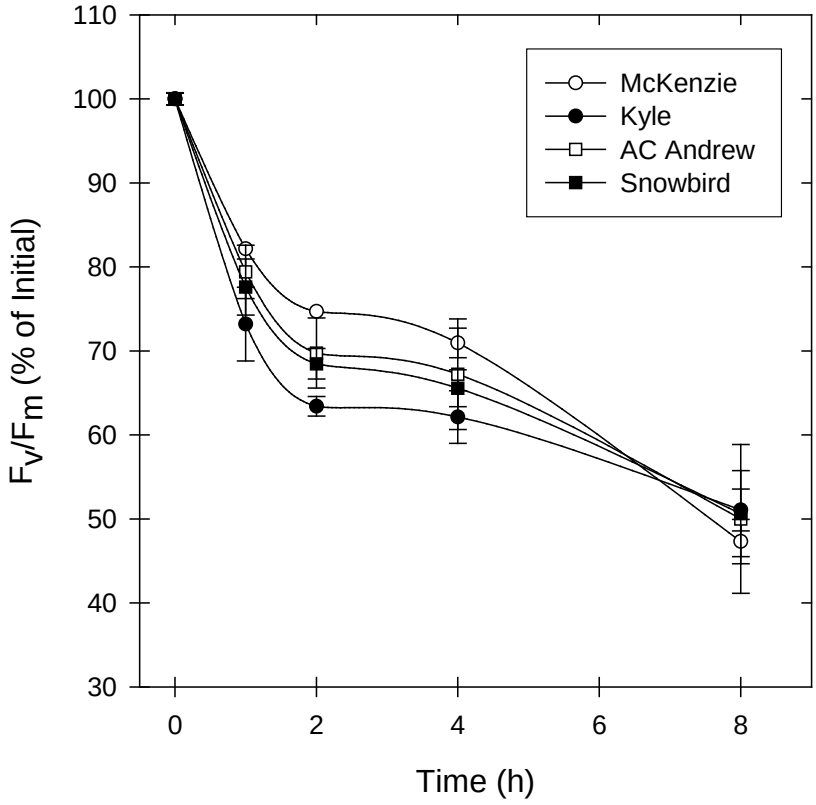

Fig. 3.2. Photoinhibitory responses estimated by the Chl fluorescence parameter F_V/F_M in various cultivars of wheat grown in field experiments for the calendar year 2008. Values represent the means ± SD, $n = 3$. When not present error bars are smaller than symbol size.

cycle carotenoids remained similar among the cultivars in response to photoinhibition, the xanthophyll cycle was clearly active as demonstrated by the 87 to 92% decrease in the EPS for all cultivars (Table 3.4). Of note was a lower xanthophyll pool size (11 to 25%) and engagement state for the AC Andrew cultivar in comparison to the others (Table 3.4).

3.4 Discussion

Field-grown plants from the 2007 growing year were apparently more resistant to photoinhibition than plants from 2008. This may be attributable to lower amounts of precipitation in the 2008 growing season. Interestingly, NDVI values were somewhat lower during 2008 which may also reflect the environmental conditions (Table 3.1). Another photoinhibition study in field-grown wheat found a 40-50% drop in F_V/F_M in only 3 h under similar photoinhibitory conditions (Yang *et al*., 2006). Studies on chamber-grown winter rye and wheat have found a decrease in F_V/F_M of up to 50% over an 8 h photoinhibitory treatment (Hurry, *et al.* 1992).

Estimates of crop biomass and yield (photosynthesis) are frequently required in breeding programs as well as for crop management applications. This study investigated these parameters in the field for a range of spring wheat cultivars commonly grown in Saskatchewan. Two non-destructive techniques, Chl fluorescence and leaf spectral reflectance, as well as CO_2 gas exchange was used for this purpose. In addition, wheat straw composition was also determined using a fiber detergent analysis method. While cellulose can be hydrolyzed into readily-fermentable glucose, hemicellulose and lignin cannot and are antagonistic to the fermentation process. High lignin content makes the fermentation process of lignocellulosic biomass into ethanol difficult (Sun and Cheng, 2002). In fact, it has also been shown that lignin and cellulose contents are inversely proportional (Sun and Cheng, 2002; Baucher *et al.*, 1999). This means that high lignin content would also mean low cellulose content. Therefore, the ideal plant for fermentation would have minimal amounts of lignin. From studying the composition analysis data, it is clear that some varieties (Kyle, AC Vista, AC Crystal) have higher lignin and lower cellulose content than other varieties (McKenzie, 5700PR, AC Avonlea). It can be concluded that some varieties show a slight advantage over others in composition for energy purposes. However, these slight differences are unlikely to prove significant during ethanol production. Overall, under field conditions there were very few differences between cultivars currently

produced in Saskatchewan and the Prairies in terms of their photosynthetic performance. While some cultivars exhibited photosynthetic traits which were improved over others, these differences are small and not likely to contribute to large change in biomass. This was verified based on DW accumulation and biomass composition. Other field studies have found that an increase in NPQ by the induction of Z and A have directly increased photoinhibitory resistance and it is likely a similar process is occurring in the cultivars examined in this study (Martinez-Ferri, 2004 *et al.*; Lu, 2001 *et al.*; Lu *et al.*, 2003). Compared to the other cultivars, AC Andrew had significantly lower zeaxanthin concentration after photoinhibition. However this did not appear to diminish its photoinhibitory resistance. Thus, none of the cultivars examined present any advantage to a producer interested in using their crop for alternative energy purposes.

4.0 PHOTOSYNTHESIS UNDER CONTROLLED ENVIRONMENTAL CONDITIONS

4.1 Introduction

Current data indicates the earth's climate is rapidly changing. Among the most prevalent is the rise in atmospheric carbon dioxide due to fossil fuel emissions. Current atmospheric concentration is in the range of 375-400 μmol mol^{-1} but is expected to rise to 600 μmol mol^{-1} as early as 2050 (Zeng *et al.* 2004). An effect of this change will be an increase in global temperature as well as severe day/night fluctuations. An increase in CO_2 could also alter plant metabolism by perturbing Rubisco carboxylation and photosynthetic balance.

Studies performed by forced-air CO_2 enrichment (FACE) indicate that plants grown above ambient CO_2 will accumulate more carbon biomass (Ainsworth and Long, 2005). C_3 plants have been shown to be especially responsive to increased CO_2 as Rubisco's carboxylation reaction is heavily favoured to the oxygenation reaction, decreasing photorespiration. This is also due to increased substrate for Rubisco which leads to elevated photosynthetic rates. Other direct benefits are increased water use efficiency due to decreased stomatal conductance/frequency and increased carboxylation and electron transport rates (Ainsworth and Long, 2005; Alonso *et al*., 2009). Correlations have been shown between photoinhibitory tolerance and CO_2 growth regime. Plants grown in high CO_2 tend to be more photosynthetically resilient compared to those grown in ambient air (Hymus et al. 2001a, Gutiérrez et al. 2009).

Cold acclimation is growth and development at low, non-freezing temperatures to acquire eventual freezing tolerance. In this process, plants must undergo photosynthetic adjustment to low/freezing temperature (Huner *et al.*, 1998; Ensminger *et al.*, 2006). Acclimation usually begins with low temperature stress and results with a plant more metabolically fit for future cold and photoinhibitory stress. The plant usually does this by increasing the abundance and activity of Calvin cycle enzymes (Strand *et al.*, 1999; Hurry *et al.*, 2000). Cold acclimated plants have been shown to be more resistant to photoinhibition than non acclimated plants (Hurry *et al*., 1995).

The purpose of this study is to characterise the photosynthesis of wheat cultivars grown in non-acclimating, cold-acclimating, high CO_2/non-acclimating and high CO_2/cold-acclimating conditions. Light and CO_2 curves will be performed to determine carbon assimilation rate as well as other modelled values. Photochemical efficiency (F_V/F_M) and xanthophyll conversion

(zeaxanthin induction) will be monitored during photoinhibitory stress. HPLC methods will be used to calculate epoxidation state (EPS) which is a relative index of xanthophylls converted to zeaxanthin. Data obtained should give insight into photosynthetic performance of these wheat cultivars under a variety of growth regimes.

4.2 Materials and methods

4.2.1 Plant material

Five wheat (*Triticum* spp.) cultivars from five market varieties were selected for study based on results from preliminary field trials. These cultivars were chosen for further analyses based on differing photoinhibitory responses and biomass characteristics (chapter 3.0). CDC Raptor was also chosen for further study as it is a winter wheat and has different responses during cold acclimation (Hurry and Huner, 1992). Seeds were sown in coarse vermiculate in 10 cm pots at a density of five seeds/pot and were irrigated with Hoagland nutrient solution as needed (Gray *et al.*, 1996). Plants were grown at ambient CO_2 in Conviron E8H and PGR15 controlled environment chambers (Conviron, Winnipeg MB) at 20°C and 5°C, respectively. Irradiance was provided by fluorescent lights at 250 µmol m^{-2} s^{-1} PPFD and a 16/8 h light/dark cycle. Plants were also grown at 750 µmol mol^{-1} CO_2 under similar conditions in a GCW15 Conviron environmental growth chamber (Chargin Falls, OH, USA) using a CO_2 injector monitored by a WMA-4 infrared CO_2 analyzer (PP Systems International, Inc. Amesbury, MA, USA. Plants were grown from seed and sampled at second fully-expanded leaf stage which took 9,11, 60 and 80 days in non acclimated/high CO_2, non acclimated/ambient CO_2, cold acclimated/high CO_2 and cold acclimated/ambient CO_2 growth regimes, respectively. Seeds were obtained from the Crop Development Centre at the University of Saskatchewan (Saskatoon SK).

4.2.2 Measurements of CO_2 exchange

CO_2 gas exchange was determined as described previously in section *3.2.5* with some exceptions. *A/Q* curve measurements had CO_2 concentrations (C_i) ranging from 190-550 µmol mol^{-1} over the course of the experiment. Humidity of incoming air was controlled at 1.6-2.5 kPa *vpdL* based on T_{leaf} which ranged from 19.7-21.3 °C, resulting in humidity values of 20-57%.
A/C$_i$ curves were constructed with C_i values ranging from to 48 to 845 µmol mol^{-1}. Humidity of incoming air was controlled at 1.5-3.4 kPa *vpdL* based on T_{leaf} which ranged from 19.8-21.4°C

during the experiment, resulting in humidity values of 15-47%.

4.2.3 Spectral Reflectance

Reflectance measurements of NDVI and PRI were performed as described in section *3.2.6.*

4.2.4 Chlorophyll fluorescence

Measurements of Chl fluorescence occurred as described in section *3.2.7.*

4.2.5 Low-temperature photoinhibition

Photoinhibition was performed as described in section *3.2.8.*

4.2.6 Pigment extraction and determination

Photosynthetic pigments wee extracted and determined as described previously in section *3.2.9.*

4.3 Results

4.3.1 Software-modelled values from light and CO_2 response curves.

To estimate certain photosynthetic values, modelling software was used (Tables 4.1-4.5, Fig B1). In light saturated curves, A_{max} averages ranged between 20 and 26 μmol CO_2 m^{-2} s^{-1} for all non acclimated and non acclimated/high CO_2 cultivars. In most cases, A_{max} values were almost 40-50% lower when grown in cold acclimated and cold acclimated/high CO_2 growth regimes. An exception is AC Andrew where A_{max} dropped 70% in cold acclimated/high CO_2 grown leaves. Light compensation averages ranged between 12 and 23 μmol m^{-2} s^{-1} in all non acclimated plants and all saw a 2-8 fold increase when grown in cold-acclimating conditions. Light saturation points did not seem to vary much throughout cultivars or growth regimes but there were some exceptions. In McKenzie light saturation points increased almost 30% when cold acclimated. In Kyle and Snowbird, cold-acclimation at ambient CO_2 caused 30 and 50% decreases in light saturation points. Φ_a seemed to be highest in cold acclimated/ambient CO_2 but no other clear trend was observed between cultivars. Dark respiration levels varied throughout all cultivars and environmental treatments between -0.63 ± 0.38 and -3.35 ± 0.62 μmol CO_2 m^{-2} s^{-1}. In most cases R_1 was highest in plants that were cold acclimated.

Table 4.1. Photosynthetic parameters of Mckenzie wheat derived from modeled light- (*A/Q*) and CO_2-response (A/C_i) curves in controlled chamber experiments. Values represent means ± SD, (n = 3).

Photosynthetic Parameter	Non-Acc.	Cold-Acc.	Non-Acc./High CO_2	Cold-Acc./High CO_2
A_{max} (µmol CO_2 m^{-2} s^{-1})	20.73 ± 2.69	16.27 ± 3.49	25.93 ± 0.31	18.13 ± 3.44
ϕ_a CO_2 (µmol CO_2/µmol photons)	0.26 ± 0.11	0.47 ± 0.03	0.16 ± 0.01	0.28 ± 0.03
Light compensation point (µmol m^{-2} s^{-1})	15.73 ± 2.08	39.13 ± 5.38	20.5 ± 2.79	73.32 ± 2.17
Light saturation point (µmol m^{-2} s^{-1})	290.67 ± 42.03	444 ± 32.51	381 ± 12.29	465.5 ± 47.6
R_1 (µmol CO_2 m^{-2} s^{-1})	-1.19 ± 0.18	-1.35 ± 0.23	-1.48 ± 0.21	-3.35 ± 0.62
A_{max} (µmol CO_2 m^{-2} s^{-1})	38.57 ± 3.41	72.5 ± 12.22	45.63 ± 5.26	51.33 ± 4.93
CE (mol CO_2 m^{-2} s^{-1})	0.32 ± 0.03	0.20 ± 0.02	0.35 ± 0.09	0.15 ± 0.01
Resp (µmol CO_2 m^{-2} s^{-1})	-9.95 ± 0.69	-10.62 ± 2.77	-10.76 ± 2.41	-12.08 ± 2.01
Γ (µmol CO_2 mol^{-1})	42.24 ± 0.39	70.66 ± 2.96	40.86 ± 2.57	100.38 ± 14.41
$V_{c,max}$ (µmol m-2 s-1)	42.6 ± 2.31	52.7 ± 12.33	48.1 ± 2.26	43.4 ± 2.69
J_{max} (µmol m-2 s-1)	113.67 ± 15.04	208 ± 27.5	132.33 ± 9.61	156.73 ± 3.33
TPU (µmol m-2 s-1)	7.32 ± 0.76	13.3 ± 1.61	10.09 ± 1.97	10.35 ± 0.73
Transpiration rate (mmol H_2O m^{-2} s^{-1})	3.49 ± 0.52	2.84 ± 0.71	2.6 ± 0.07	2.66 ± 0.53
Stomatal conductance (mol m^{-2} s^{-1})	0.19 ± 0.03	0.10 ± 0.03	0.40 ± 0.06	0.12 ± 0.04
Intrinsic water use efficiency (µmol CO_2 mmol H_2O^{-1})	4.83 ± 0.5	3.98 ± 0.72	7.61 ± 0.04	3.67 ± 0.54

Table 4.2. Photosynthetic parameters of Kyle wheat derived from modeled light- (*A/Q*) and CO_2-response (A/C_i) curves in controlled chamber experiments. Values represent means ± SD, (n = 3).

Photosynthetic Parameter	Non-Acc.	Cold-Acc.	Non-Acc./High CO_2	Cold-Acc./High CO_2
A_{max} (µmol CO_2 m^{-2} s^{-1})	24.27 ± 4.27	14.8 ± 1.71	20.8 ± 2.13	14.08 ± 2
ϕ_a CO_2 (µmol CO_2/µmol photons)	0.48 ± 0.07	0.88 ± 0.10	0.51 ± 0.06	0.26 ± 0.06
Light compensation point (µmol m^{-2} s^{-1})	13.3 ± 1.75	26.67 ± 7.37	12.39 ± 2.11	62.2 ± 6.27
Light saturation point (µmol m^{-2} s^{-1})	366 ± 39.04	222.33 ± 22.72	312 ± 14.11	408.53 ± 20.34
R_1 (µmol CO_2 m^{-2} s^{-1})	-0.91 ± 0.11	-1.73 ± 0.18	-0.82 ± 0.2	-2.52 ± 0.38
A_{max} (µmol CO_2 m^{-2} s^{-1})	44.00 ± 3	34.7 ± 2.01	37.87 ± 1.81	32.01 ± 5.07
CE (mol CO_2 m^{-2} s^{-1})	0.31 ± 0.06	0.09 ± 0.02	0.38 ± 0.04	0.17 ± 0.05
Resp (µmol CO_2 m^{-2} s^{-1})	-9.22 ± 1.98	-7.81 ± 1.75	-10.1 ± 1.08	-7.83 ± 0.8
Γ (µmol CO_2 mol^{-1})	37.21 ± 2.86	67.81 ± 1.18	40.17 ± 0.38	72.25 ± 9.18
$V_{c,max}$ (µmol m-2 s-1)	51.86 ± 9.37	31.33 ± 2.2	39.8 ± 4.36	33.66 ± 4.45
J_{max} (µmol m-2 s-1)	134.33 ± 7.57	107 ± 7	108 ± 6	90.52 ± 9.85
TPU (µmol m-2 s-1)	10.14 ± 0.83	6.26 ± 0.79	8.74 ± 0.45	5.8 ± 0.6
Transpiration rate (mmol H_2O m^{-2} s^{-1})	4.14 ± 0.73	3.47 ± 0.14	3.98 ± 0.43	2.14 ± 0.45
Stomatal conductance (mol m^{-2} s^{-1})	0.24 ± 0.06	0.12 ± 0.00	0.24 ± 0.04	0.09 ± 0.02
Intrinsic water use efficiency (µmol CO_2 mmol H_2O^{-1})	4.72 ± 0.4	3.35 ± 0.22	4.35 ± 0.14	4.26 ± 0.52

Table 4.3. Photosynthetic parameters of AC Andrew wheat derived from modeled light- (A/Q) and CO_2-response (A/C_i) curves in controlled chamber experiments. Values represent means ± SD, (n = 3).

Photosynthetic Parameter	Non-Acc.	Cold-Acc.	Non-Acc./High CO_2	Cold-Acc./High CO_2
A_{max} (µmol CO_2 m^{-2} s^{-1})	22.93 ± 1.86	13.93 ± 1.01	22.63 ± 1.01	6.8 ± 1.93
ϕ_a CO_2 (µmol CO_2/µmol photons)	0.27 ± 0.06	0.74 ± 0.10	0.38 ± 0.07	0.27 ± 0.04
Light compensation point (µmol m^{-2} s^{-1})	17.5 ± 0.72	39.63 ± 10.49	12.77 ± 0.75	103.1 ± 16.95
Light saturation point (µmol m^{-2} s^{-1})	326.33 ± 18.5	365 ± 27.84	326 ± 27.62	331 ± 37.32
R_1 (µmol CO_2 m^{-2} s^{-1})	-1.3 ± 0.05	-1.81 ± 0.38	-0.84 ± 0.09	-2.06 ± 0.29
A_{max} (µmol CO_2 m^{-2} s^{-1})	37.9 ± 1.39	41.1 ± 3.73	39.37 ± 3.98	85.53 ± 9.35
CE (mol CO_2 m^{-2} s^{-1})	0.27 ± 0.01	0.14 ± 0.02	0.24 ± 0.05	0.08 ± 0.02
Resp (µmol CO_2 m^{-2} s^{-1})	-7.96 ± 0.77	-5.99 ± 0.69	-6.77 ± 2.34	-9.5 ± 1.77
Γ (µmol CO_2 mol^{-1})	38.79 ± 3.26	50.04 ± 10.17	40.07 ± 0.99	143.12 ± 9.67
$V_{c,max}$ (µmol m-2 s-1)	42.67 ± 11.33	36.1 ± 5.12	68.9 ± 3.8	35.37 ± 6.85
J_{max} (µmol m-2 s-1)	114 ± 4.36	122.33 ± 25.93	84.7 ± 11.59	114.2 ± 28.88
TPU (µmol m-2 s-1)	7.3 ± 0.18	8.06 ± 1.69	10.73 ± 0.5	9.65 ± 2.09
Transpiration rate (mmol H_2O m^{-2} s^{-1})	3.87 ± 0.15	2.41 ± 0.98	3.25 ± 0.81	1.04 ± 0.3
Stomatal conductance (mol m^{-2} s^{-1})	0.21 ± 0.01	0.11 ± 0.01	0.21 ± 0.07	0.05 ± 0.02
Intrinsic water use efficiency (µmol CO_2 mmol H_2O^{-1})	4.53 ± 0.32	5.33 ± 1.53	4.96 ± 0.33	3.61 ± 0.3

Table 4.4. Photosynthetic parameters of Snowbird wheat derived from modeled light- (*A/Q*) and CO_2-response (*A/C*$_i$) curves in controlled chamber experiments. Values represent means ± SD, (*n* = 3).

Photosynthetic Parameter	Non-Acc.	Cold-Acc.	Non-Acc./High CO_2	Cold-Acc./High CO_2
A_{max} (µmol CO_2 m^{-2} s^{-1})	24.37 ± 0.64	14.7 ± 1.41	20.63 ± 0.67	11.83 ± 0.25
ϕ_a CO_2 (µmol CO_2/µmol photons)	0.16 ± 0.03	0.89 ± 0.02	0.27 ± 0.01	0.28 ± 0.06
Light compensation point (µmol m^{-2} s^{-1})	15.73 ± 0.85	10.62 ± 3.18	14.53 ± 1.63	73.6 ± 9.34
Light saturation point (µmol m^{-2} s^{-1})	317 ± 26.06	148.67 ± 27.02	294 ± 11.79	495.67 ± 10.97
R_1 (µmol CO_2 m^{-2} s^{-1})	-1.27 ± 0	-1.2 ± 0.53	-1.05 ± 0.07	-1.84 ± 0.08
A_{max} (µmol CO_2 m^{-2} s^{-1})	45.93 ± 0.46	51.3 ± 5.38	40.27 ± 0.93	32.21 ± 0.58
CE (mol CO_2 m^{-2} s^{-1})	0.30 ± 0.02	0.15 ± 0.04	0.26 ± 0.03	0.18 ± 0.02
Resp (µmol CO_2 m^{-2} s^{-1})	-9.38 ± 0.47	-8.56 ± 1.76	-8.6 ± 0.83	-10.19 ± 0.19
Γ (µmol CO_2 mol^{-1})	38.89 ± 0.79	68.00 ± 2.47	42.14 ± 0.99	85.57 ± 6.12
$V_{c,max}$ (µmol m-2 s-1)	45.83 ± 0.72	43.97 ± 6.23	39.5 ± 0.53	29.57 ± 0.15
J_{max} (µmol m-2 s-1)	142.67 ± 0.58	158.33 ± 22.03	119 ± 1.73	92.01 ± 1.67
TPU (µmol m-2 s-1)	9.09 ± 0.12	12.6 ± 1.54	9.39 ± 0.73	6.95 ± 0.47
Transpiration rate (mmol H_2O m^{-2} s^{-1})	4.14 ± 0.28	3.16 ± 0.72	3.88 ± 0.1	2.16 ± 0.13
Stomatal conductance (mol m^{-2} s^{-1}	0.23 ± 0.02	0.12 ± 0.05	0.25 ± 0.01	0.12 ± 0.01
Intrinsic water use efficiency (µmol CO_2 mmol H_2O^{-1})	4.51 ± 0.19	4.11 ± 0.49	4.34 ± 0.06	3.62 ± 0.15

Table 4.5. Photosynthetic parameters of CDC Raptor wheat derived from modeled light- (A/Q) and CO_2-response (A/C_i) curves in controlled chamber experiments. Values represent means ± SD, (n = 3).

Photosynthetic Parameter	Non-Acc.	Cold-Acc.	Non-Acc./High CO_2	Cold-Acc./High CO_2
A_{max} (µmol CO_2 m^{-2} s^{-1})	20.83 ± 1.87	11.86 ± 2.75	26.57 ± 3.73	10.76 ± 0.43
ϕ_a CO_2 (µmol CO_2/µmol photons)	0.25 ± 0.03	0.35 ± 0.06	0.22 ± 0.03	0.26 ± 0.02
Light compensation point (µmol m^{-2} s^{-1})	16.1 ± 1.65	66.97 ± 11.13	22.8 ± 3.58	88.9 ± 7.51
Light saturation point (µmol m^{-2} s^{-1})	319.33 ± 18.82	454 ± 82.93	341.33 ± 14.29	383.93 ± 40.03
R_1 (µmol CO_2 m^{-2} s^{-1})	-1.04 ± 0.21	-0.63 ± 0.38	-2.04 ± 0.22	-3.25 ± 0.19
A_{max} (µmol CO_2 m^{-2} s^{-1})	35.37 ± 2.92	47.83 ± 5.05	49.03 ± 0.15	62.03 ± 12.03
CE (mol CO_2 m^{-2} s^{-1})	0.30 ± 0.09	0.11 ± 0.05	0.33 ± 0.01	0.11 ± 0.02
Resp (µmol CO_2 m^{-2} s^{-1})	-9.14 ± 2.38	-9.45 ± 2.21	-9.35 ± 1.43	-9.65 ± 2.13
Γ (µmol CO_2 mol^{-1})	40.07 ± 1.48	68.79 ± 4.44	35.04 ± 6.12	112.81 ± 2.07
$V_{c,max}$ (µmol m-2 s-1)	35.73 ± 3.52	40.4 ± 6.09	48.03 ± 0.32	40.06 ± 5.58
J_{max} (µmol m-2 s-1)	104 ± 3.61	145.33 ± 23.5	156 ± 2.65	115.2 ± 35.03
TPU (µmol m-2 s-1)	7.06 ± 0.15	15.6 ± 1.54	10.35 ± 1.52	6.84 ± 1.93
Transpiration rate (mmol H_2O m^{-2} s^{-1})	3.77 ± 0.28	1.89 ± 0.60	2.89 ± 0.06	1.27 ± 0.14
Stomatal conductance (mol m^{-2} s^{-1}	0.26 ± 0.02	0.08 ± 0.05	0.41 ± 0.03	0.06 ± 0.01
Intrinsic water use efficiency (µmol CO_2 mmol H_2O^{-1})	4.35 ± 0.62	3.72 ± 1.38	7.67 ± 0.26	4.58 ± 0.15

Stomatal conductance was 2-fold higher in non acclimated plants compared to cold acclimated plants when grown at ambient CO_2. However when grown at high CO_2, stomatal conductance was 3-4 fold higher in non acclimated plants. In both cases increases in stomatal conductance lead to increased water transpiration rates. However when transpiration rate is corrected for carbon assimilation rate, water use efficiency is similar (Kyle, AC Andrew) or higher (McKenzie, CDC Raptor, Snowbird).

Curves for saturating CO_2 were also modelled using similar software (Tables 4.1-4.5). A_{max} in this case, was found to be similar throughout cultivars and growth regimes and most were between 32.01 ± 5.1 and 51.3 ± 5.4 μmol CO_2 $m^{-2}s^{-1}$. McKenzie however, had a two-fold increase when cold acclimated at ambient CO_2, while AC Andrew had the same increase when cold acclimated at high CO_2. CE averaged between 0.24 ± 0.05 and 0.38 ± 0.04 mol CO_2 m^{-2} s^{-1} in non acclimated and non acclimated high CO_2 plants. These values dropped 30-60% when cold acclimated and varied between ambient and high CO_2 grown-plants. Resp was usually the same throughout all growth regimes in CDC Raptor, Snowbird, Kyle and McKenzie with averaged values between -7.81 ± 1.75 and -12.08 ± 2.01. AC Andrew grown at non-acclimating/ambient CO_2 was found to have a 20% drop in Resp when cold acclimated and when grown at high CO_2. CO_2 compensation points were usually double when comparing cold acclimated to non acclimated plants at ambient CO_2. However, at high CO_2, AC Andrew and CDC Raptor had CO_2 compensation values that were 3-fold higher in cold acclimated plants.

Carboxylation rates were not significantly affected by growth regime in CDC Raptor and McKenzie. In the other cultivars, cold acclimation decreased carboxylation rates by as much as 20%. Growth in high CO_2 also increased carboxylation by 50% in AC Andrew when non acclimated. Conversely, Snowbird had decreased carboxylation rates at high CO_2 when cold acclimated. J_{max} did not significantly change in Kyle, AC Andrew, Snowbird and CDC Raptor and averaged between 84.7 ± 11.59 and 158.33 ± 22.03 μmol $m^{-2}s^{-1}$. McKenzie however had an electron transport rate of 208 ± 27.5 μmol $m^{-2}s^{-2}$ when cold acclimated at ambient CO_2. Triose phosphate utilization was highest under cold-acclimating/ambient CO_2 conditions except for Kyle. Conversely, TPU was the lowest when cold acclimated and at high CO_2.

4.3.2 Photochemical efficiency before and after photoinhibition.

Prior to photoinhibitory stress on wheat leaves, initial measurements were taken (Table

4.6). Initial values of F_V/F_M in non acclimated wheat were 0.77 ± 0.01 -0.79 ± 0.01 for all cultivars before photoinhibitory stress was applied, while cold acclimated cultivars ranged between 0.66 ± 0.01 and 0.74 ± 0.02. When grown at non acclimated/high CO_2 and cold acclimated/high CO_2, these values did not change much with values of 0.78 ± 0.01-0.80 ± 0.01 and 0.61 ± 0.02-0.72 ± 0.02, respectively.

As a measure of plant productivity, NDVI reflectance measurements were used. NDVI is calculated from the absorbance and reflectance of two different wavelength of light and has been used previously as and index of chlorophyll content (Gamon and Surfus, 1999). NDVI values fluctuated between all cultivars with no clear trend in each growth regime with averages between 0.44 ± 0.05 and 0.72 ± 0.01. In McKenzie, Kyle and AC Andrew the lowest NDVIs were found in cold acclimated/high CO_2 grown wheat. However, in Snowbird and CDC Raptor, the lowest NDVIs were found in plants grown in non acclimated/high CO_2 growth regime. In general, the highest NDVI were found in the non acclimated/ambient CO_2 plants.

Resistance to photoinhibitory stress is a good indicator of photosynthetic vigour (Long *et al*., 1994). After 8 h of photoinhibitory stress were applied, non acclimated/ambient CO_2 plants were found to be the least resistant (Table 4.6, Figure 4.1). Decrease in F_V/F_M for non acclimated plants was between 36 and 55% from initial values. The only exception is AC Andrew where non-acclimated/high CO_2 was found to decrease the most out of all growth regimes at an average of 46%. Other non acclimated/high CO_2 plants were also found to be weakly resistant to photoinhibition ranging between 39.5 ± 5.35 and 47.04 ± 3.48%. Cold acclimated and cold acclimated/high CO_2 plants had decreases of 16.24 ± 0.74-26.67 ± 1.2% and 3.06 ± 3.13 -24.43 ± 3.52 %. AC Andrew and Snowbird both had average drops of a mere 3% in F_V/F_M in these cold acclimated/high CO_2 leaves. This represents the most resistant cultivars and growth regime. Most cultivars saw the most dramatic decrease after 6 h of photoinhibition (Figure 4.1). After 4 h photoinhibition, all cultivars had a slight recovery in F_V/F_M compared to after 2 h photoinhibition in cold acclimated high CO_2 plants.

4.3.3 Xanthophyll pigment quantification during photoinhibition.

As a result of photoinhibitory stress, photosynthetic xanthophyll pigments are induced (Demmig-Adams and Adams, 1996). HPLC analysis was performed on the entire second fully-

Table 4.6. Maximal fluorescence yield of PSII (F_V/F_M) and NDVI of wheat cultivars before photoinhibition. Also tabulated is the % drop in F_V/F_M after 8 h photoinhibition. Values represent means ± SD, (n = 3).

Market Variety	Cultivar	Growth regime	F_V/F_M	NDVI	% Drop F_V/F_M
Canada Western Red Spring	McKenzie	Non-Acc.	0.78 ± 0.01	0.69 ± 0.01	50.62 ± 2.22
		Cold-Acc.	0.74 ± 0.02	0.65 ± 0.02	20.24 ± 3.85
		Non-Acc./High CO_2	0.79 ± 0.01	0.62 ± 0.05	39.5 ± 5.35
		Cold-Acc./High CO_2	0.72 ± 0.02	0.44 ± 0.05	12.47 ± 2.54
Canada Western Amber Durum	Kyle	Non-Acc.	0.77 ± 0.01	0.57 ± 0.03	49.57 ± 1.35
		Cold-Acc.	0.66 ± 0.01	0.50 ± 0.05	16.24 ± 0.74
		Non-Acc./High CO_2	0.79 ± 0.01	0.64 ± 0.03	47.04 ± 3.48
		Cold-Acc./High CO_2	0.66 ± 0.02	0.66 ± 0.01	10.99 ± 4.55
Canada Western Soft White Spring	AC Andrew	Non-Acc.	0.77 ± 0.01	0.72 ± 0.01	36.64 ± 0.47
		Cold-Acc.	0.72 ± 0.01	0.67 ± 0.03	20.73 ± 1.11
		Non-Acc./High CO_2	0.79 ± 0.00	0.69 ± 0.02	45.99 ± 6.37
		Cold-Acc./High CO_2	0.61 ± 0.02	0.48 ± 0.08	3.27 ± 1.68
Canada Western Hard White Spring	Snowbird	Non-Acc.	0.77 ± 0.00	0.71 ± 0.01	55.84 ± 1.3
		Cold-Acc.	0.75 ± 0.00	0.67 ± 0.02	26.67 ± 1.2
		Non-Acc./High CO_2	0.80 ± 0.01	0.59 ± 0.05	55.23 ± 3.77
		Cold-Acc./High CO_2	0.65 ± 0.02	0.62 ± 0.02	3.06 ± 3.13
Canada Western Red Winter	CDC Raptor	Non-Acc.	0.78 ± 0.01	0.69 ± 0.01	47.24 ± 1.33
		Cold-Acc.	0.71 ± 0.02	0.57 ± 0.03	22.03 ± 3.13
		Non-Acc./High CO_2	0.78 ± 0.01	0.54 ± 0.04	40.86 ± 3.5
		Cold-Acc./High CO_2	0.72 ± 0.01	0.61 ± 0.03	24.43 ± 3.52

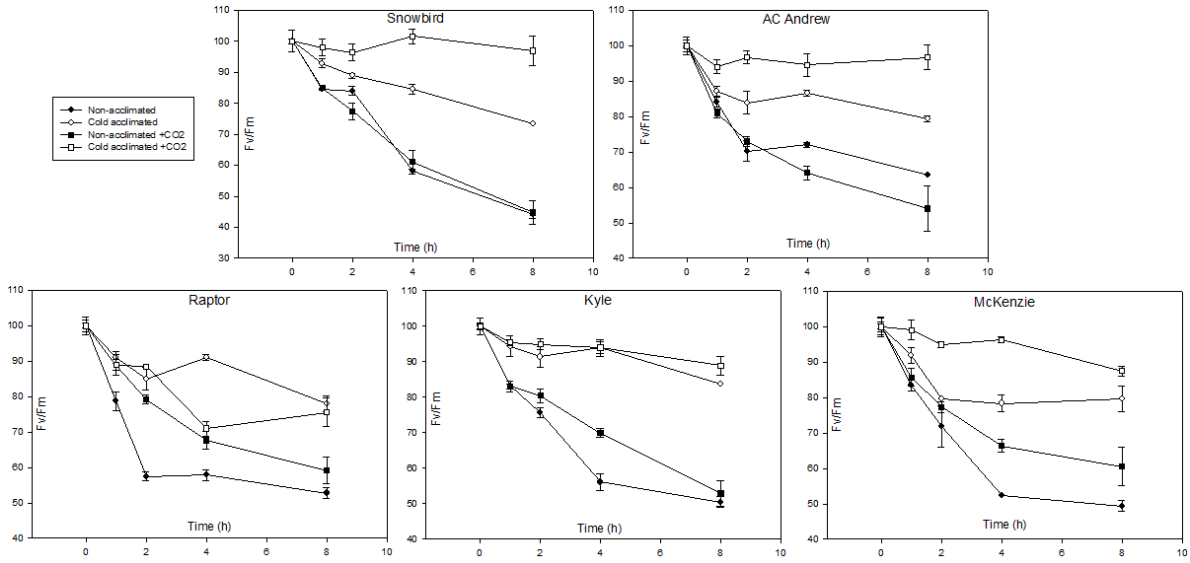

Fig. 4.1. Photoinhibitory responses estimated by the Chl fluorescence parameter F_V/F_M in various cultivars of wheat grown in controlled environment chambers. Values represent the means ± SD, *n* = 3 as a percentage of F_V/F_M prior to photoinhibition. When not present, error bars are smaller than symbol size.

expanded leaf (Tables 4.7-4.11). β-carotene levels varied between cultivars but did not seem to be affected by growth regime or photoinhibitory treatment. Lutein levels were not visibly affected by photoinhibitory treatment but were usually the lowest in non acclimated/ambient CO_2 and even lower in non acclimated/high CO_2 growth regime. Also there is no clear relationship between neoxanthin levels and photoinhibition/growth regime as values fluctuate.

The most drastic differences are observed when observing the changes in violaxanthin, antheraxanthin and zeaxanthin during photoinhibition. Upon photoinhibition, violaxanthin is converted into antheraxanthin and eventually, zeaxanthin as a photoprotectant. In most cultivars, the total pool size of these three pigments (V+A+Z) is the same before and after 8 h photoinhibition. However, the greatest pool sizes are found in plants grown in ambient CO_2 under both non and cold-acclimating conditions. In cold acclimated Kyle and AC Andrew, the total pool is size is respectively 15 and 40% larger when compared to plants grown in cold acclimated/high CO_2.

Before photoinhibition, Zeaxanthin is very low compared to Violaxanthin or not even detected. After photoinhibition, the inverse is true. The 8 h photoinhibition was drastic enough to nearly convert all Violaxanthin into Antheraxanthin and Zeaxanthin. Post-inhibition, Antheraxanthin increased 3- to 4-fold in all cultivars and growth regimes. The most drastic examples of Zeaxanthin induction are shown under cold-acclimating/ambient CO_2 conditions. Additionally, Zeaxanthin induction was also comparatively high in non-acclimating/ambient conditions compared to those grown in high CO_2. Minimal differences were seen between cultivars.

Two other ways to monitor the xanthophyll cycle is by monitoring EPS and PRI (Table 4.12). EPS is reflected in the de-epoxidation of zeaxanthin from the V+A+Z pool. The higher the EPS value the more zeaxanthin is induced. In almost all cases, EPS before photoinhibition averaged between 0.91 ± 0.06 and 0.99 ± 0.04. The exception is non acclimated/ambient CO_2 AC Andrew which has an EPS of 0.74 ± 0.04. This is due to high zeaxanthin levels in these samples. After photoinhibition, all samples EPS dropped between 0.90 and 0.71. EPS values appear to directly relate to zeaxanthin concentration. Values for PRI also increased during photoinhibition in all cultivars. Although PRI changed with EPS, it was not consistent and seemed to increase to varying amounts throughout cultivars and growth regimes.

Table 4.7. Photosynthetic pigment content of McKenzie wheat grown in controlled chamber experiments. Plants were grown under controlled growth regimes as indicated and analyzed pre-and post-photoinhibition. Values represent means ± SD, (n = 3).* Not detected.

Cultivar	β-C	L	N	V	A	Z	V+A+Z
(mmol mol^{-1} Chl a+b)							
Pre-Photoinhibition							
Non-Acc.	96.13 ± 12.73	148.01 ± 20.48	34.41 ± 4.28	46.71 ± 4.3	1.58 ± 0.13	nd*	48.28 ± 4.88
Cold-Acc.	61.8 ± 7.08	94.57 ± 12.44	46.63 ± 5.73	46.12 ± 6.14	4.06 ± 0.53	2.6 ± 0.19	52.77 ± 7.54
Non-Acc./High CO_2	63.43 ± 4.37	141.29 ± 9.66	24.08 ± 3.02	31.59 ± 3.28	3.61 ± 0.35	nd	35.2 ± 3.99
Cold-Acc./High CO_2	67.98 ± 4.41	185.7 ± 15.17	12.38 ± 0.8	37.23 ± 4.44	5.81 ± 0.34	0.7 ± 0.08	43.74 ± 5.35
Post-Photoinhibition (8h)							
Non-Acc.	111.9 ± 6.46	112.64 ± 11.77	14.7 ± 1.31	Nd	9.34 ± 0.56	44.98 ± 3.17	54.32 ± 4.1
Cold-Acc.	59.48 ± 7.51	123.53 ± 14.18	50.51 ± 4.97	Nd	12.67 ± 0.7	48.68 ± 4.92	61.35 ± 6.17
Non-Acc./High CO_2	51.82 ± 2.64	130.38 ± 12.75	7.04 ± 0.65	Nd	11.13 ± 1.03	31.46 ± 2.88	42.58 ± 4.3
Cold-Acc./High CO_2	73.06 ± 8.3	176.3 ± 9.94	4.27 ± 0.58	Nd	13.84 ± 1.81	44.24 ± 2.65	58.08 ± 4.9

Table 4.8. Photosynthetic pigment content of Kyle wheat grown in controlled chamber experiments. Plants were grown under controlled growth regimes as indicated and analyzed pre-and post-photoinhibition. Values represent means ± SD, (n = 3).* Not detected.

Cultivar	β-C	L	N	V	A	Z	V+A+Z
(mmol mol^{-1} Chl a+b)							
Pre-Photoinhibition							
Non-Acc.	45.21 ± 4.33	153.96 ± 17.68	24.24 ± 3.04	63.13 ± 5.63	2.27 ± 0.3	0.01 ± 0.9	65.4 ± 5.4
Cold-Acc.	80.97 ± 7.52	107.73 ± 13.32	19.16 ± 1.81	75.75 ± 4.26	3.96 ± 0.53	1.15 ± 0.66	80.86 ± 9.21
Non-Acc./High CO_2	66.72 ± 4.13	102.19 ± 7.52	17.17 ± 1.02	43.62 ± 2.5	4.23 ± 0.43	0.02 ± 0.39	47.85 ± 7.57
Cold-Acc./High CO_2	68.01 ± 5.13	123.21 ± 7.47	24.03 ± 1.2	35.71 ± 4.54	3.31 ± 0.24	0.5 ± 0.6	39.52 ± 10.73
Post-Photoinhibition (8h)							
Non-Acc.	79.94 ± 6.75	151.59 ± 14.33	15.28 ± 1.69	2.6 ± 0.28	9.84 ± 0.87	53.37 ± 2.84	65.82 ± 4.39
Cold-Acc.	72.94 ± 7.37	123.2 ± 16.74	16.84 ± 1.1	nd*	20.12 ± 1.19	68.23 ± 2.29	88.35 ± 3.82
Non-Acc./High CO_2	47.88 ± 3.14	85.45 ± 4.8	10.17 ± 1.15	0.74 ± 0.06	13.92 ± 1.31	36.76 ± 2.53	51.41 ± 4.3
Cold-Acc./High CO_2	70.22 ± 5.74	169.73 ± 22.88	14.69 ± 0.87	Nd	12.44 ± 1.45	23.05 ± 2.32	35.49 ± 4.15

Table 4.9. Photosynthetic pigment content of AC Andrew wheat grown in controlled chamber experiments. Plants were grown under controlled growth regimes as indicated and analyzed pre-and post-photoinhibition. Values represent means ± SD, (n = 3). * Not detected.

Cultivar	β-C	L	N	V	A	Z	V+A+Z
(mmol mol^{-1} Chl a+b)							
Pre-Photoinhibition							
Non-Acc.	68.65 ± 5.79	90.01 ± 6.14	17.89 ± 2.42	40.42 ± 5.52	2.93 ± 0.17	13.39 ± 8.11	56.74 ± 9.67
Cold-Acc.	84.24 ± 7.75	130.86 ± 16.04	16.03 ± 1.35	89.71 ± 7.61	6.63 ± 0.45	4.06 ± 0.94	100.39 ± 8.2
Non-Acc./High CO_2	85.07 ± 6.64	84.49 ± 8.23	21.95 ± 2.91	46.75 ± 4.37	3.31 ± 0.24	0.00 ± 0.75	50.06 ± 10.03
Cold-Acc./High CO_2	67.2 ± 5.31	100.75 ± 5.56	21.94 ± 1.86	43.29 ± 3.57	2.98 ± 0.34	0.48 ± 0.58	46.75 ± 10.64
Post-Photoinhibition (8h)							
Non-Acc.	97.84 ± 8.9	101.23 ± 8.47	8.73 ± 0.54	0.38 ± 0.05	10.79 ± 0.7	47.24 ± 1.29	58.4 ± 2.24
Cold-Acc.	81.95 ± 6.9	159.04 ± 10.13	7.57 ± 0.57	3.47 ± 0.22	13.5 ± 1.54	71.27 ± 2.32	88.25 ± 4.47
Non-Acc./High CO_2	67.2 ± 4.1	74.28 ± 4.06	12.01 ± 1.59	Nd	13.67 ± 1.08	40.96 ± 2.67	54.62 ± 4.13
Cold-Acc./High CO_2	72.67 ± 4.46	124.34 ± 9.46	16.77 ± 1.38	Nd	11.64 ± 0.6	36.24 ± 1.98	47.88 ± 2.84

Table 4.10. Photosynthetic pigment content of Snowbird wheat grown in controlled chamber experiments. Plants were grown under controlled growth regimes as indicated and analyzed pre-and post-photoinhibition. Values represent means ± SD, (n = 3). *Not detected.

Cultivar	β-C	L	N	V	A	Z	V+A+Z
(mmol mol^{-1} Chl a+b)							
Pre-Photoinhibition							
Non-Acc.	49 ± 3.22	141.33 ± 12.76	20.74 ± 2.81	69.52 ± 7.05	3.09 ± 0.42	1.31 ± 0.07	73.92 ± 8.29
Cold-Acc.	65.2 ± 3.27	149.02 ± 12.88	25.31 ± 1.52	52.55 ± 4.88	7.44 ± 0.74	7.17 ± 0.81	67.15 ± 7.07
Non-Acc./High CO_2	55.33 ± 6.24	87.58 ± 8.57	23.89 ± 1.67	52.5 ± 2.69	4.38 ± 0.52	0.01 ± 0.49	56.88 ± 8.89
Cold-Acc./High CO_2	51.8 ± 3.36	151.23 ± 8.64	14.85 ± 1.17	39.99 ± 5.58	3.12 ± 0.29	0.62 ± 0.7	43.73 ± 8.7
Post-Photoinhibition (8h)							
Non-Acc.	41.95 ± 5.75	171.79 ± 10.12	20.07 ± 2.18	0.58 ± 0.06	10.36 ± 1.45	63.57 ± 7.11	74.51 ± 9.48
Cold-Acc.	45.57 ± 4.97	138.49 ± 12.46	11.17 ± 1.17	nd*	19.84 ± 2.14	56.27 ± 3.31	76.11 ± 6
Non-Acc./High CO_2	51.73 ± 3.29	96.74 ± 12.29	8.72 ± 1.14	11.29 ± 1.35	12.59 ± 1.39	44.8 ± 3.88	68.68 ± 7.29
Cold-Acc./High CO_2	60.17 ± 3.94	165.35 ± 21.63	7.43 ± 0.59	Nd	9.18 ± 0.61	35.34 ± 1.2	44.51 ± 1.99

Table 4.11. Photosynthetic pigment content of CDC Raptor wheat grown in controlled chamber experiments. Plants were grown under controlled growth regimes as indicated and analyzed pre-and post-photoinhibition. Values represent means ± SD, (n = 3). *Not detected.

Cultivar	β-C	L	N	V	A	Z	V+A+Z
(mmol mol^{-1} Chl a+b)							
Pre-Photoinhibition							
Non-Acc.	46.1 ± 5.23	118.66 ± 6.46	4.02 ± 0.48	62.2 ± 7.69	1.93 ± 0.18	2.15 ± 0.84	66.28 ± 11.24
Cold-Acc.	64.59 ± 4.17	147.54 ± 13	17.7 ± 2.34	74.9 ± 8.61	1.87 ± 0.2	2.17 ± 1.11	78.95 ± 12.05
Non-Acc./High CO_2	68.32 ± 6.74	88.41 ± 8.99	24.46 ± 1.64	56.72 ± 7.19	1.26 ± 0.1	0.10 ± 0.89	57.98 ± 10.15
Cold-Acc./High CO_2	54.86 ± 6.02	120.33 ± 12.79	29.12 ± 1.74	34.55 ± 3.93	2.13 ± 0.23	1.91 ± 0.59	38.59 ± 11.07
Post-Photoinhibition (8h)							
Non-Acc.	58.88 ± 7.59	116.85 ± 13.16	13.13 ± 1.29	nd*	9.86 ± 0.52	52.69 ± 1.82	62.55 ± 2.57
Cold-Acc.	78.62 ± 6.14	143.24 ± 13.19	13.89 ± 1.92	Nd	9.24 ± 0.67	65.98 ± 2.6	75.22 ± 3.6
Non-Acc./High CO_2	72.5 ± 9.87	78.88 ± 7.1	12.74 ± 0.94	1.93 ± 0.25	10.08 ± 0.51	43.93 ± 1.69	55.94 ± 2.69
Cold-Acc./High CO_2	60.88 ± 7.25	122.06 ± 14.59	4.12 ± 0.47	Nd	10.55 ± 1.34	33.78 ± 1.81	44.33 ± 3.46

Table 4.12. Comparison of EPS and PRI of wheat grown in controlled environment chamber before and after photoinhibition. Δ PRI and Δ EPS are based on increase in PRI and EPS after 8 h photoinhibition as monitored by HPLC analysis and a hand-held reflectometer. Values were determined on second fully-expanded leaf. Values represent means ± SD, (n = 3).

Cultivar	Growth regime	PRI (0h)	EPS (0h)	PRI (8h)	EPS (8h)
McKenzie	Non-Acc.	-0.33 ± 0.06	0.98 ± 0.05	0.22 ± 0.02	0.09 ± 0.05
	Cold-Acc.	-0.25 ± 0.02	0.91 ± 0.06	-0.36 ± 0.05	0.1 ± 0.03
	Non-Acc./High CO_2	-0.3 ± 0.16	0.95 ± 0.04	0.02 ± 0.07	0.13 ± 0.03
	Cold-Acc./High CO_2	-0.12 ± 0.04	0.92 ± 0.05	0.41 ± 0.1	0.12 ± 0.03
Kyle	Non-Acc.	-0.37 ± 0.03	0.98 ± 0.05	0.13 ± 0.03	0.11 ± 0.05
	Cold-Acc.	-0.49 ± 0.06	0.96 ± 0.04	0.53 ± 0.09	0.11 ± 0.05
	Non-Acc./High CO_2	-0.27 ± 0.1	0.96 ± 0.02	0.09 ± 0.02	0.15 ± 0.05
	Cold-Acc./High CO_2	-0.28 ± 0.17	0.95 ± 0.05	0.07 ± 0.15	0.18 ± 0.04
AC Andrew	Non-Acc.	-0.28 ± 0.04	0.74 ± 0.04	0.26 ± 0.03	0.1 ± 0.06
	Cold-Acc.	-0.45 ± 0.06	0.93 ± 0.03	0.18 ± 0.12	0.12 ± 0.03
	Non-Acc./High CO_2	-0.27 ± 0.06	0.97 ± 0.04	-0.13 ± 0.06	0.13 ± 0.04
	Cold-Acc./High CO_2	-0.19 ± 0.06	0.96 ± 0.05	0.24 ± 0.02	0.12 ± 0.06
Snowbird	Non-Acc.	-0.29 ± 0.02	0.96 ± 0.03	0.23 ± 0.07	0.08 ± 0.05
	Cold-Acc.	-0.45 ± 0.05	0.84 ± 0.04	-0.36 ± 0.13	0.13 ± 0.04
	Non-Acc./High CO_2	-0.31 ± 0.12	0.96 ± 0.06	0.00 ± 0.1	0.26 ± 0.05
	Cold-Acc./High CO_2	-0.1 ± 0.04	0.95 ± 0.05	0.31 ± 0.03	0.1 ± 0.03
CDC Raptor	Non-Acc.	-0.28 ± 0.07	0.95 ± 0.04	0.06 ± 0.02	0.08 ± 0.04
	Cold-Acc.	-0.49 ± 0.06	0.96 ± 0.04	-0.19 ± 0.03	0.06 ± 0.05
	Non-Acc./High CO_2	-0.27 ± 0.06	0.99 ± 0.04	-0.11 ± 0.25	0.12 ± 0.04
	Cold-Acc./High CO_2	-0.41 ± 0.07	0.92 ± 0.03	0.19 ± 0.06	0.12 ± 0.05

4.4 Discussion

Five common Saskatchewan cultivars from five different market varieties were studied under four different environmental conditions. Although these cultivars differ in appearance and end-product use, minimal differences were observed in their photosynthetic performance. The most drastic difference seen in this study is the difference between wheat grown and acclimated in different growth regimes. This is expected as plants grown in different temperatures and CO_2 concentrations often undergo photosynthetic and metabolic perturbations (Huner *et al.*, 1993; Ainsworth and Long, 2005; Ensminger *et al.*, 2006). Varying degrees of decreases in F_V/F_M during photoinhibition can mostly be explained by modelled values from light and CO_2 response curves.

Wheat that was grown in ambient CO_2 and non-acclimating conditions was the least photoinhibitory resistant out of the four growth regimes. The average decrease in F_V/F_M throughout the 8 h treatment was between 36 and 55%. It has been shown that development at lower excitation pressure does not allow plants to become photoinhibitory tolerant (Gray *et al.*, 1996). This is probably not due to a decrease in zeaxanthin induction as most plants had similar EPS and PRI values before and after photoinhibition. Zeaxanthin induction was also usually highest in these plants and therefore is not the only factor in photoinhibitory resistance. The difference probably lies with its carbon metabolism. In all non acclimated cultivars CE and are much higher than those that are cold acclimated. This is reflected in higher A_{max} values and CO_2 and light compensations points. Additionally, TPU rate was usually lowest in these non acclimated/ambient CO_2 cultivars. A decrease in the rate of TPU means a decrease in the ability for a plant to handle excess phosphorylated intermediates in the Calvin cycle during photoinhibitory stress (Savitch *et al.*, 2000). This is probably the main reason for the poor photoinhibitory resistance of wheat grown in this growth regime.

When these cultivars are cold acclimated, drastic differences in their responses to photoinhibition are shown. Under ambient CO_2, the decrease in F_V/F_M was only between 16 and 26%. This was due to these plants developing under higher excitation pressure (Gray *et al.*, 1996). A complete reprogramming of carbon metabolism allowed for a higher TPU rate in most cultivars. However these plants had much more conservative photosynthesis when carbon assimilation was recorded. CO_2 assimilation curves were taken at room temperature. Because these plants were still acclimated to 5 C°, stomatal conductance was very low. For probably this

reason, A_{max} was the lowest in cold acclimated plants while CO_2 saturating and compensation points were higher. Because cold acclimated plants are usually limited by temperature, placement into a warmer regime makes these plants Rubisco limited. Xanthophyll pool size (V+A+Z) was also much higher in plants grown in this growth regime, possibly leading to increased photoprotection.

It was observed that photoinhibitory resistance was only slightly higher when grown at high CO_2 and non-acclimating conditions. Some cultivars (Snowbird, Kyle) had photoinhibitory responses, as monitored by decrease in F_V/F_M, which were identical to their ambient CO_2 counterpart. This is also reflected in identical photosynthetic parameters in the light and CO_2 response curves. AC Andrew however showed a decrease in photoinhibitory resistance compared to ambient CO_2 although TPU and carboxylation rate was higher. This could be explained by the fact that electron transport rate was lower when grown at high CO_2 as shown previously (Alonso *et al.*, 2009). Conversely, CDC Raptor and Mckenzie had increased photoinhibitory resistance when grown at high CO_2. These cultivars had concomitant changes in A_{max}, J_{max}, TPU and $V_{c,max}$. Increased activity or expression of Calvin cycle enzymes is believed to account for this (Alonso *et al*., 2009).

With the exception of CDC Raptor, all cold acclimated plants had increased photoinhibitory resistance when grown at high CO_2. With AC Andrew and Snowbird, average photoinhibitory resistance increased 4- and 7-fold, respectively. No photosynthetic values derived from the light and CO_2 curves seem to account for this. In all cultivars, CE, Φ_a, carboxylation rate, TPU, electron transport rate is the same or lower. This phenomenon can also not be explained by xanthophyll induction as EPS changes and xanthophyll pool sizes are lower than those grown in cold acclimated/ambient CO_2.

It is clear that although many of these cultivars differ in photosynthetic responses to photoinhibition, the major disparities are environmental. Each growth regime has different strategies to combat high-light/low temperature stress. Under ambient CO_2, cold-acclimation leads to increased xanthophyll pool size and TPU. This leads to increased triose-phosphate processing, which in turn, decreases excitation pressure. Plants grown at high CO_2 do not differ in xanthophyll induction but some differ in carboxylation rate, TPU and J_{max}. These changes could account for the increase in photoinhibitory resistance as high CO_2 has been shown to increase photosynthetic rates (Harley and Sharkey, 1992; Ainsworth and Long, 2005). The ability

for plants to adjust to high CO_2 is satisfactory in a world of increasing CO_2 concentration.

5. GENERAL DISCUSSION

5.1 Contrasting field and non acclimated wheat

In the crop year of 2008 Mckenzie, Kyle, AC Andrew and Snowbird were grown in the field. Field-grown wheat from 2008 had similar photochemical efficiencies as those grown under non-acclimating/ambient CO_2 conditions. Also, they also had comparable photoinhibitory resistance. During the 8 h treatment as most plants had decreases in F_V/F_M of about 50%, similar to wheat grown in non-acclimating conditions. Xanthophyll induction was also indistinguishable in plants from both growth regimes. NDVI values were also similar.

However, drastic differences are seen between field-grown plants and all other chamber plants based on the light and CO_2 curves. Field-grown wheat had A_{max} values that were 1.5 to 2 fold higher than their non acclimated, chamber-grown counterpart. Light compensation and saturation points were at least half in field-grown wheat. CE was double in all cultivars except for Mckenzie which was actually tripled in field-conditions. Carboxylation efficiency and TPU was usually at least double in field-grown wheat. Averages for J_{max} were 2.5-4 fold higher in Snowbird and Mckenzie, respectively. Stomatal conductance was also 1.5 fold higher in field-grown plants.

Based on these observations, field-grown wheat has a much higher photosynthetic capacity that non acclimated wheat. Increased carboxylation, electron transport and sugar metabolism allows for increased rates of photosynthesis. Irradiance of a Saskatchewan summer can be 10-fold the irradiances (possibly photoinhibitory) in the environmental chambers used in this study. The temperature is also constantly changing. Because field-grown wheat thrives in a much more variable and comparatively hostile environment, it needs a much more productive photosynthesis. In a way, it is acclimated to these harsh field conditions. Surprisingly, acclimation to comparatively extreme irradiances does not improve their photoinhibitory resistance or their relative xanthophyll pool size. CO_2 assimilation curves were also taken at higher temperatures (up to 29°C) in the field compared to room temperature for chamber plants. This higher temperature could account for higher metabolic and enzymatic rates leading to increased photosynthesis.

5.2 Metabolic shifts between cold acclimated and non acclimated wheat

Wheat that was grown at 5°C is referred to as cold acclimated and was shown to have

increased resistance to photoinhibition as compared to non acclimated wheat. This is due to metabolic differences between plants from both growth regimes. Although CE decreased in cold acclimated plants, carboxylation rates ($V_{c,max}$) increased in most cultivars. An increase in overall carboxylation rates refers to either increased activity or abundance of Rubisco. An increase in Rubisco activity has also been described by Hurry *et al.* (1995, 2000) in cold acclimated winter rye and *Arabidopsis*. Cold acclimation has been also characterised by increased expression of sucrose phosphate synthase and fructose-1,6-bisphosphatase leading to increased sugar phosphate pools. This allows for increased concentration of substrate for the Calvin cycle enzymes and allows for their further activation. This trend is reflected in this study as TPU rates are higher in most cultivars. In the case of CDC Raptor and Mckenzie, TPU rate increased 2-fold when cold acclimated. These data indicate that photosynthesis in cold acclimated spring and winter wheat is capable of elevated metabolic flux. Because low temperatures limit enzymatic processes, the plant must find a way to overcome this limitation.

Cold-acclimation is also associated with increased electron transport rates (Hurry *et al*., 1993). Maximal electron transport rates were shown to significantly increase in Mckenzie and CDC Raptor but remained unchanged in the other cultivars when cold acclimated. This is probably due to an inherent ability for these cultivars to either increase PQ levels or to keep them continually oxidized. However, this capacity would allow for increased photoinhibitory tolerance over the other cultivars and is not perceived in this study.

It appears Mckenzie and CDC Raptor has a higher capacity to adjust to low temperature metabolically. Conversely, Kyle seems to be the least able to properly cold-acclimate. Carboxylation, electron transport and TPU rates actually decreased upon cold-acclimation but did not seem to affect its photoinhibitory resistance. Perhaps other cold-acclimation metabolic changes not examined in this study are better indicators of photoinhibitory resistance.

5.3 Metabolic shifts between ambient and high CO_2 grown wheat

Under non-acclimating conditions, CO_2 concentration is the limiting factor in photosynthesis. Previous work in this field has demonstrated that C_3 plants, when grown at elevated CO_2 concentrations, have increased photosynthetic capacity and biomass accumulation (Harley and Sharkey, 1991; Hymus *et al.*, 2001a, 2001b; Alonso *et al.*, 2008; Gutiérrez *et al*., 2009). The simplest reason for increased photosynthesis rates is that Rubisco is substrate (CO_2)

saturated which increases the carboxylation and competitively inhibits the oxygenation reaction. In this study however, plants were grown at high CO_2 but had photosynthetic rates measured at ambient CO_2. In this way, acclimation to high CO_2 can be studied without substrate-saturating Rubisco.

Studies have found that acclimation to high CO_2 concentrations increases photochemistry by increasing J_{max} and overall yield of photosystem II (Hymus *et al*., 2001a, 2001b). This is due to the fact that increased carboxylation causes a shift in electron flux to photosynthesis rather than the carbon oxidation cycle. In Mckenzie and CDC Raptor, A_{max}, $J_{max\ and}$ $V_{c,max}$ have all increased under non-acclimating conditions in ambient CO_2. Along with increased photosynthesis, TPU is also increased, leading to increased carbon flux through the Calvin cycle (Harley and Sharkey, 1991). This could allow for the increased resistance to photoinhibition seen in these cultivars.

Snowbird, AC Andrew and Kyle grown at high CO_2, did not show increased photosynthetic rates. It has been shown that C_3 plants have increased photochemical quenching during photoinhibitory treatment (Hymus *et al*., 2001a; Gutiérrez *et* al., 2009). Photochemical quenching allows dissipation of excess energy from PSII to PSI. In this case, plants grown at high CO_2 are able to quench excess irradiance without down-regulating photosynthesis or inducing the xanthophyll cycle. This is reflected in this study as all high CO_2 plants had decreased zeaxanthin induction as well as xanthophyll pool size.

Under cold-acclimating conditions no significant photosynthetic changes are seen when comparing ambient to high CO_2 grown wheat. In most cases, A_{max} has actually decreased. This could be due to a down-regulation in photosynthesis caused by a decrease in Rubisco transcript or Rubisco enzyme activity (Alonso *et al*., 2008). It is also well accepted that increased photosynthesis due to high CO_2 acclimation is temperature dependant (Harley *et al*., 1992; Gutiérrez *et al*., 2009). This is believed to be caused by release of Rubisco inhibitors and its subsequent activation at higher temperatures. With increasing CO_2 atmospheric concentrations and global temperatures, earth could experience an adjustment in the way its plant life assimilate carbon.

5.4 Relating xanthophyll pigment levels and PRI

Xanthophyll cycle induction is frequently used for dissipation of excess light energy

(Demmig-Adams and Adams, 1996). High levels of irradiance can actually be harmful to the plant when light harvesting centers of PSII absorb more light energy than can be used for the metabolic reactions of photosynthesis. This leads to an abundance of reactive oxygen species and a lower chloroplast lumen pH. This situation is known as photoinhibition and can be detrimental to the plant cell. Fortunately, plants have an immediate defence to photoinhibitory stress. Acidic lumen pH stimulates conversion of violaxanthin to antheraxanthin and zeaxanthin via the xanthophyll cycle. Zeaxanthin is considered a photoquenching pigment and is used to filter excess irradiance as well as function as an antioxidant (Johnson *et al.*, 2007). This process is known as NPQ and allows for functional photosynthesis in photoinhibitory conditions (Demmig-Adams and Adams, 1996).

Wheat in this study exhibited complete conversion of violaxanthin into zeaxanthin after an 8 h photoinhibitory period. Pigment levels were monitored by HPLC analysis. Plants grown at ambient CO_2 had the highest concentrations of zeaxanthin per cultivar. Although not drastically different, plants grown at high CO_2 had less zeaxanthin and overall xanthophyll pool size. It is evident that high CO_2 grown wheat is able to be more photoinhibitory resistant without as much use of the xanthophyll cycle for photoinhibitory tolerance. This is due to metabolic changes described in section *5.3*.

Xanthophyll conversion was also monitored by the change in PRI over the 8 h photoinhibitory treatment. PRI is a non-destructive reflectance method used to estimated zeaxanthin abundance/conversion. Induction of zeaxanthin and change in PRI (Δ PRI) only loosely correlated with one another. Cold acclimated Kyle and AC Andrew both exhibited the highest zeaxanthin concentrations as well as the largest Δ PRI. However, some examples are contradictory to this as Mckenzie has highly variable Δ PRI between environmental regimes and nearly consistent zeaxanthin concentration. According to this study, PRI results should only be used for approximation and should be confirmed with HPLC analysis.

It is evident that zeaxanthin is integral for photoinhibitory protection for spring and winter wheat. However, zeaxanthin concentration varies only slightly between cultivars and could not account for the variety of F_V/F_M decrease during photoinhibition. Metabolic activities, as discussed in sections *5.2* and *5.3*, must allow for the variety of photoinhibitory responses observed in this study.

5.5 Conclusions

Although the major differences observed in this study were between environmental regimes, some differences were noted between cultivars. Mckenzie seemed to be a photosynthetically adept cultivar. Being one of the most cultivated wheats in Western Canada, it has been economically selected from the large Canada Western Red Spring Wheat market by the producer. It has also been selected for yield by the plant breeder. The high yielding trait of Mckenzie could be assisted by its photosynthetic performance. In the field, it had the highest CO_2 assimilation rates with corresponding increases in electron transport, carboxylation rate and triose phosphate utilization. It also had low lignin and high cellulose making it ideal for lignocellulosic ethanol production. In controlled environmental chambers it was able to adequately acclimate to cold and high CO_2 conditions. This was also reflected in its photoinhibitory tolerance as acclimation in both growth regimes its vigour.

CDC Raptor is a Canada Western Red Winter wheat that is also very popular among growers. As with any good winter wheat, it readily cold and CO_2 acclimated similarly to Mckenzie. Under high CO_2 or low temperature, it had increased carboxylation, electron transport and TPU. Although it did not have the best photoinhibitory tolerance, it had adequate defence to photoinhibitory stress with high TPU and xanthophyll pool size.

Kyle acclimated well to low temperature as monitored by photoinhibitory tolerance. Kyle did not experience any photosynthetic changes from the modelled CO_2 data that indicates that it had cold acclimated. Cold acclimated and field-grown Kyle did however have an enormous xanthophyll pool size and zeaxanthin concentrations when photoinhibited. This alone could not account for increased photoinhibitory resistance when cold acclimated and probably undergoes metabolic changes not investigated in this study. Kyle, a Canada Western Amber durum cultivar, is commonly grown in the southern and warmer sections of the prairies and is probably less influenced by acclimatory performance (McCallum and DePauw, 2008). High CO_2 also did not seem to significantly improve its tolerance to high irradiance/low temperature. High lignin also makes this cultivar unsuitable for cellulosic ethanol technology.

AC Andrew is from the Canada Western Soft White Spring wheat class is commonly known for its soft, white flour. Like Kyle, it is cultivated in warmer sections of the prairies and does not cold-acclimate well in this study. Its does however, have a great capacity to acclimate to high CO_2. Although electron transport does not change, TPU and carboxylation rates increase

30% in elevated CO_2 conditions. These changes also have no effect on A_{max} but do help in its photoinhibitory tolerance. Cold acclimated/high CO_2 grown AC Andrew had one of the lowest drops in F_V/F_M during 8 h photoinhibition at only 3%.

Snowbird seemed photosynthetically indifferent to growth at high CO_2 under non-acclimating conditions. However when comparing Snowbird grown under cold-acclimating conditions, elevated CO_2 greatly improved its photoinhibitory tolerance (3% drop in F_V/F_M). This cultivar was able to do this without an increase in any photosynthetic parameter observed in this study. It can be speculated that photoinhibitory resistance can be attained with increased levels and activities of Calvin cycle enzymes leading to increased carbon flux.

This study has shown that out of the eleven spring wheat cultivars grown in the field that no one cultivar had considerable photosynthetic advantages over the others. This trend was also reflected in overall biomass accumulation in the field. However, studies in controlled environment chambers revealed major differences between wheat in different growth regimes. Development to low temperature allowed for up-regulated carbon metabolism and increased photoinhibitory tolerance. Additionally, growth at high CO_2 increased electron transport rates leading to enhanced photosynthetic capacity.

5.6 Future research

The photosynthetic and metabolic differences discussed between wheat grown in different growth regimes are supported by previous studies. Photosynthetic changes observed can be explained by other publications that looked at expression and activity of Calvin cycle enzymes, electron flux or redox status of PQ (Hurry *et al.*, 1995, 2000; Ensminger *et al.*, 2006; Alonso *et al.*, 2008). Future studies could be enzyme activity assays that could directly characterise Calvin cycle activity of wheat grown in these growth regimes. Some acclimatory metabolic changes of anomalous cultivars (discussed in 5.5) may have went unnoticed in this study (Snowbird, AC Andrew,) and this would give a broader perspective.

Photoinhibitory responses could also be better investigated by subjecting plants to NPQ slow induction kinetics. In this method, chlorophyll fluorescence is monitored over a series of saturating flashes during the first few minutes of photoinhibition. In this study, xanthophyll induction was only measured over a long time scale (8 h) by HPLC analysis. Slow induction kinetics could show differences in photoprotective responses during the first crucial moments of

photoinhibition, contributing to its understanding. Excitation pressure (1-qP) could also be calculated from these experiments. HPLC analysis could also be performed a few minutes after the photoinhibitory treatment begins. Immediate photoinhibitory differences could be seen between cultivars/environmental treatment.

This study focused on photosynthesis of the leaf. This is a limitation as leaf photosynthesis does not take into account photosynthesis/cellular respiration of other tissues. Future studies could focus on whole plant photosynthesis using a chlorophyll fluorescence camera or a sealed atmospheric chamber (Leonardos *et al.*, 2003). Alternatively, photosynthesis could be studied at the ecosystem level with the assistance of satellite NDVI and PRI measurements.

Considering that the market varieties we see today were not selected for photosynthetic performance, it would be interesting to see if there are differences in the expression of photosynthetic genes of the light harvesting complex or Calvin cycle enzymes (Ensminger *et al.*, 2006). Perhaps the more photoinhibitory resistant cultivars could have genetic markers linked to photosynthetic hardiness. If suitable genetic markers for photosynthetic hardiness were discovered, it could lead to future marker assisted breeding strategies for winter cereals. Additionally, winter cereal cultivars could be selected for winter survival success based on their photoinhibitory vigour. Cultivars with the highest winter survival ratings may also have the best strategies to winter acclimate.

6. REFERENCES

Ainsworth, E.A. and Long, S.P. (2005). What have we learned from 15 years of free-air CO_2 enrichment (FACE)? A meta-analytic review of the responses of photosynthesis, canopy properties and plant production to rising. New Phytol. *165*, 351-372.

Alonso , A., Pérez, P. and Martinez-Carrasco, R. (2009). Growth in elevated CO_2 enhances temperature response of photosynthesis in wheat. Physiol. Plantarum *135*, 109-120.

Aparicio, N., Villegas, D., Casadesus, J., Araus, J. L. and Royo, C. (2000). Spectral vegetation indices as nondestructive tools for determining durum wheat yield. Agron. J. *92*, 83-91.

Baerr, J.N., Thomas, J.D., Taylor, B.G., Rodermel, S.R. and Gray, G.R. (2005). Differential photosynthetic compensatory mechanisms exist in the *immutans* mutant of *Arabidopsis thaliana*. Physiol. Plantarum *124*, 390-402.

Baker, N.R. and Rosenqvist, E. (2004). Applications of chlorophyll fluorescence can improve crop production strategies: an examination of future possibilities. J. Exp. Bot. *55*, 1607-1621.

Baker, N.R. (2008). Chlorophyll fluorescence: a probe of photosynthesis in vivo. Annu. Rev. Plant Biol. *59*, 89-113.

Baucher, M., Bernard-vailhé, M.A., Chabbert, B., Besle, J.M., Opsomer, C, Montagu, M.V. and Botterman, J. (1999). Down-regulation of cinnamyl alcohol dehydrogenase in transgenic alfalfa (*Medicago sativa* L.) and the effect on lignin composition and digestibility. Plant Mol. Biol. *39*, 437-447.

Bernhard, K. and Grosjean, Mernahrd (1995). Infrared spectroscopy In Carotenoids v. 1B spectroscopy, Britton, G., Liaaen-Jensen, S. and Pfander, H., ed. (Birkhäuser Boston, Boston, Maryland) pp 118-134.

Buch, K., Stransky, H., Bigus, H.J. and Hager, A. (1994). Enhancement of artificial electron acceptors of thylakoid lumen acidification and zeaxanthin formation. J. Plant Physiol. *144*, 641-648.

Canadian Wheat Board. (2006). 2006 Canadian Wheat Board Variety Survey. [Online] Available: www.cwb.ca/public/en/farmers/surveys/variety/archive/pdf/2006/2006_variety_survey.pdf [2006 Oct. 10].

Clarke, J.M., Mcleod, J.M., McCaig, T.N., Depauw, R.M., Knox, R.E. and Fernandez, M.R. (1998). AC Avonlea durum wheat. Can. J. Plant Sci. *78*, 621-623.

Demmig-Adams, B. and Adams, W.W. (1992). Photoprotection and other responses of plants to high light stress. Ann. Rev. Plant. Physiol. *43*, 599-626.

Demmig-Adams, B. and Adams, W.W. (1996). The role of xanthophyll cycle carotenoids in the

protection of photosynthesis. Trends Plant Sci. *1*, 21-26.

Depauw, R.M., McCaig, T.N., Knox, R.E., Clarke, J.M., Fernandez, M.R. and McLeod, J.G. (1998). AC Vista hard white spring wheat. Can. J. Plant Sci. *78*, 617-620.

Diaz, M., Ball, E. and Lüttge, U. (1990). Stress-induced accumulation of the xanthophyll rhodoxanthin in leaves of *Aloe vera*. Plant Physiol. Biochem. *28*, 679-682.
Farquhar, G.D., Caemmerer, S. von and Berry, J.A. (1980). A biochemical model of photosynthetic CO_2 assimilation in leaves of C_3 species. Planta. *149*, 78-90.

Fernandez, M.R., DePauw, R.M., Knox, R.E., Clarke, J.M., McCaig, T.N. and McLeod, J.G. (1998). AC Crystal red spring wheat. Can. J. Plant Sci. *78*, 307-310.

Fowler, D.B. (1997). CDC Clair winter wheat. Can. J. Plant Sci. *77*, 669-671.

Fowler, D.B. (1999). CDC Falcon winter wheat. Can. J. Plant Sci. *79*, 599-601.

Fowler, D.B. (2002). CDC Raptor winter wheat. Can. J. Plant Sci. *82*, 407-409.

Ensminger, I., Busch, F. and Huner, N.P.A. (2006). Photostasis and cold acclimation: sensing low temperature through photosynthesis. Physiol. Plantarum *126*, 28-44.

Evans, L.E., Shebeski, L.H., McGinnis, R.C., Briggs, K.G. and Zuzenz, D. (1972). Glenlea red spring wheat. Can. J. Plant Sci. *52*, 1081-1082.

Gamon, J.A. and Surfus, J.S. (1999). Assessing leaf pigment content and activity with a reflectometer. New Phytol. *143*, 105-117.

García-Plazaola, J.I. and Becerril, J.M. (1999). A rapid high-performance liquid chromatography method to measure lipophilic antioxidants in stressed plants: simultaneous determination of carotenoids and tocopherols. Phytochem. Analysis *10*, 307-313.

Graf, R.J., Hucl, P., Orshinsky, B.R. and Kartha, K.K. (2003). McKenzie hard red spring wheat. Can. J. Plant Sci. *83*, 565- 569.

Gray, G.R., Savitch, L.V., Ivanov, A.G. and Huner, N.P.A. (1996). Photosystem II excitation pressure and development of resistance to photoinhibition II. Adjustment of photosynthetic capacity in winter wheat and winter rye. Plant Physiol. *110*, 61-71.

Gray, G.R., Hope, B.J., Qin, X., Taylor, B.G. and Whitehead, C.L. (2003). The characterization of photoinhibition and recovery during cold acclimation in *Arabidopsis thaliana* using chlorophyll fluorescence imaging. Physiol. Plantarum. *119*, 365-375.

Gutiérrez, D., Gutiérrez, E., Pérez, P., Morcuende, R., Verdejo, A.L. and Martinez-Carrasco, R. (2009). Acclimation to future atmospheric CO_2 levels increases photochemical efficiency and mitigates photochemistry inhibition by warm temperatures in wheat under field chambers.

Physiol. Plantarum 137, *86*-100.

Harbinson, J., Genty, B. and Baker, N.R. (1990). The relationship between CO_2 assimilation and electron transport in leaves. Photosyn. Res. *25*, 213-224.

Harley, P.C., Thomas, R.B., Reynolds, J.F. and Strain B.R. (1992). Modelling photosynthesis of cotton grown in elevated CO_2. Plant Cell Environ. *15*, 271-282.

Harley, P.C. and Sharkey, T.D. (1991). An improved model of C_3 photosynthesis at high CO_2: reversed O_2 sensitivity explained by lack of glycerate reentry into the chloroplast. Photosyn. Res. *27*, 169-178.

Holm, G. (1954). Chlorophyll mutations in barley. Acta Agric. Scand. *4*, 457-471.

Holt, N.E., Zigmantas, D., Valkunas, L., Li, X.P., Niyogi, K.K. and Fleming, G.R. (2005). Carotenoid cation formation and the regulation of photosynthetic light harvesting. Science *307*, 433–436.

Humphries, D.G., Townley-Smith, T.F., Czarnecki, E., Lukow, O.M., McCallum, B., Fetch, T., Gilbert, J. and Menzies, J. (2007). Snowbird hard red spring wheat. Can. J. Plant Sci. *87*, 301-305.

Huner, N.P.A., Öquist, G., Hurry, V.M., Krol, M., Falk, S. and Griffith, M. (1993). Photosynthesis, photoinhibition and low temperature acclimation in cold tolerant plants. Photosyn. Res. *37*, 19-39.

Huner, N.P.A, Öquist, G. and Sarhan, F. (1998). Energy balance and acclimation to light and cold. Trends Plant Sci. *3*, 224-230.

Hurry, V.M., Gardeström, P. and Öquist, G. (1992). Reduced sensitivity to photoinhibition following frost-hardening of winter rye is due to increased phosphate availability. Planta *190*, 484-490.

Hurry, V.M. and Huner, N.P.A. (1992). Effect of cold hardening on sensitivity of winter and spring wheat leaves to short-term photoinhibition and recovery of photosynthesis. Plant Physiol. *100*, 1283-1290.

Hurry, V.M., Gardeström, P. and Öquist, G. (1993). Reduced sensitivity to photoinhibition following frost-hardening of winter rye is due to increased phosphate availability. Planta. *190*, 484-490.

Hurry, V.M., Keerberg, O., Pärnik, T., Gardeström, P. and Öquist, G. (1995). Cold-hardening results in increased activity of enzymes involved in carbon metabolism in leaves of winter rye (*Secale cereale* L.). Planta. *195*, 554-562.

Hurry, V., Strand, Å., Furbank, R. and Stitt, M. (2000). The role of inorganic phosphate in the

development of freezing tolerance and the acclimation of photosynthesis to low temperature is revealed by the *pho* mutants of *Arabidopsis thaliana*. Plant J. *24*, 383-396.

Hymus, G.J., Baker, N.R. and Long S.P. (2001a). Growth in elevated CO_2 can both increase and decrease photochemistry and photoinhibition of photosynthesis in a predictable manner. dactylis glomerata grown in two level of nitrogen nutrition. Plant Physiol. *127*, 1204-1211.

Hymus, G.J., Dijkstra, P., Baker, N.R., Drake, B.G. and Long S.P. (2001b). Will rising CO_2 protect plants from the midday sun? A study of photoinhibition of *Quercus myrtifolia* in a scrub-oak community in two seasons. Plant Cell Environ. *24*, 1361-1368.

Ireland, C.R., Long, S.P. and Baker, N.R. (1989). An integrated portable apparatus for the simultaneous field measurements of photosynthetic CO_2 and water vapour exchange, light absorption and chlorophyll fluorescence emission of attached leaves. Plant Cell Environ. *12*, 947-958.

Johnson, M.P., Havaux, M., Triantaphylides, C., Ksas, B., Pascal, A.A., Robert, B., Davison, P.A., Ruban, A.V. and Horton, P. (2007). Elevated zeaxanthin bound to oligomeric LHCII enhances the resistance of Arabidopsis to photo-oxidative stress by a lipid-protective, anti-oxidant mechanism. J. Biol. Chem. *282*, 22605-22618.

Krause, G.H and Weis E. (1991). Chlorophyll fluorescence and photosynthesis: the basics. Annu. Rev. Plant Physiol. Plant Mol. Biol. *42*, 313-319.

Leonardos, E.D., Savitch, L.V., Huner, N.P.A., Öquist, G. And Grozdinski, B. (2003). Daily photosynthetic and C-export patterns in winter wheat leaves during cold stress and acclimation. Physiol. Plant. *117*, 521-531.

Long, S.P., Humphries, S. and Falkowski, P.G. (1994). Photoinhibition of photosynthesis in nature. Annu. Rev. Plant Physiol. Plant Mol. Biol. *45*, 633–662.

Lu, C., Lu, Q., Zhang, J. and Kuang, T. (2001). Characterization of photosynthetic pigment composition, photosystem II photochemistry and thermal energy dissipation during leaf senescence of wheat plants grown in the field. J. Exp. Bot. *52*, 1805-1810.

Lu, Q., Wen, X, Lu, C., Zhang, Q. and Kuang, T. (2003). Photoinhibition and photoprotection in senescent leaves of field-grown plants. Plant Physiol. Biochem. *41*, 749-754.

Malkin, R. and Niyogi, K. (2000). Photosynthesis. In Biochemistry and molecular biology of plants, Buchanan, B.B., Gruissem, W. and Jones, R.L., ed. (American Society of Plant Biologists, Rockville, Maryland), pp. 568-628.

Martinez-Ferri, E., Manrique, E., Valladeres, F. and Balague, L. (2004). Winter photoinhibition in the field involves different processes in four co-occuring Mediterranean tree species. Tree Physiol. *24*, 981-990.

Maxwell, K., Johnson, G.N. (2000). Chlorophyll fluorescence-a practical guide. J. Exp. Bot. *51*, 659-668.

McCaig, T.N., DePauw, R.M., Clarke, J.M., McLeod, J.G., Fernandez and Knox, R.E. (1996). AC Barrie hard red spring wheat. Can. J. Plant Sci. *76*, 337-339.

McCallum, B.D. and Depauw, R.M. (2008). A review of wheat cultivars grown in the Canadian prairies. Can. J. Plant Sci. *88*, 649-677.

Nelson, D.L. and Cox, M.M. (2005). Carbohydrate biosynthesis in plants and bacteria. In Lehninger principles of biochemistry, (W.H. Freeman and Company, New York, New York), pp. 754-762.

Olsson, T. and Leverenz, J.W. (1994). Non-uniform stomatal closure and the apparent convexity of the photosynthetic photon flux density response curve. Plant Cell Environ. *17*, 701-710.

Osmond, C.B. and Grace, S.C. (1995). Perspectives on photoinhibition and photorespiration in the field: quintessential inefficiencies of the light and dark reactions of photosynthesis? J. Exp. Bot. *46*, 1351-1362.

Parsons, R., Weyers, J.D.B., Lawson, T. and Godber, I.M. (1997). Rapid and straightforward estimates of photosynthetic characteristics using a portable gas exchange system. Photosynthetica *34*, 265-279.

Pfannschmidt, T. (2003). Chloroplast redox signals: how photosynthesis controls its own genes. Trends Plant Sci. *8*, 33-41.

Poore, M.H., Moore, J.A., Swingle, R.S., Eck, T.P. and Brown W.H. (1991). Wheat straw or alfalfa hay in diets with 30% neutral detergent fiber for lactating Holstein cows. J. Dairy Sci. *74*, 3152-3159.

Prasad, B., Babar, M.A., Carver, B.F., Raun, W.R. and Klatt, A.R. (2009). Association of biomass production and canopy spectral reflectance indices in winter wheat. Can. J. Plant Sci. *89*, 485-496.

Prioul JL and Chartier P. (1977). Partitioning of transfer and carboxylation components of intracellular resistance to photosynthetic CO_2 fixation: A critical analysis of the methods used. Ann Bot-London *41*, 789-800.

Rohacek, K. (2002). Chlorophyll fluorescence parameters: the definitions, photosynthetic meaning, and mutual relationships. Photosynthetica *40*, 13-29.

Sadasivaiah, R.S., Perkovic, S.M., Pearson, D.C., Postman, B. and Beres, B.L. (2004). Registration of AC Andrew wheat. Crop Sci. *44*, 696-697.

Sane, V.S., Ivanov, A.G., Hurry, V., Huner, N.P.A. and Öquist, G. (2003). Changes in the redox

potential of primary and secondary electron-accepting quinones in photosystem II confer increased resistance to photoinhibition in low-temperature-acclimated *Arabidopsis*. Plant Phys. *132*, 2144-2151.

Savitch, L.V., Gray, G.R. and Huner, N.P.A. (1997). Feedback-limited photosynthesis and regulation of sucrose-starch accumulation during cold acclimation and low-temperature stress in a spring and winter wheat. Planta *201*, 18-26.

Savitch, L.V., Barker-Åstrom, J., Ivanov, A.G., Hurry, V., Öquist, G., Huner, N.P.A. and Gardeström, P. (2001). Cold acclimation of *Arabidopsis thaliana* results in incomplete recovery of photosynthetic capacity, associated with an increased reduction of chloroplast stroma. Planta. *214*, 295-303.

Seaton, G.R. and Walker D.A. (1990). Chlorophyll fluorescence as a measure of photosynthetic carbon assimilation. Proc. Royal Soc. Lond. B *242*, 29-35.

Somersalo, S. and Krause, G.H. (1990). Reversible photoinhibition of unhardened and cold acclimated spinach leaves at chilling temperatures. Planta. *180*, 181-187.

Stitt, M., Hurry, V. (2002). A plant for all seasons: alterations in photosynthetic carbon metabolism during cold acclimation in *Arabidopsis*. Curr. Opin. Plant Biol. *5*, 199–206.

Strand, Å., Hurry, V., Gustafsson, P. and Gardeström, P. (1997). Development of Arabidopsis thaliana leaves at low temperatures releases the suppression of photosynthesis and photosynthetic gene expression despite the accumulation of soluble carbohydrates. Plant J. *123*, 605-614.

Strand, Å., Hurry, V., Henkes, F., Huner, H., Gustaffson, P., Gardeström, P. and Stitt, M. (1999). Acclimation of *Arabidopsis* leaves developing at low temperatures. Increasing cytoplasmic volume accompanies increase activities of enzymes in the Calvin cycle and in the sucrose-biosynthesis pathway. Plant Physiol. *199*, 1387-1397.

Stylinski, C.D., Gamon, J.A. and Oechel, W.C. (2002). Seasonal patterns of reflectance indices, carotenoid pigments and photosynthesis of evergreen chaparral species. Oecologia *131*, 366-374.

Sun, Y. and Cheng, J. (2002). Hydrolysis of lignocellulosic materials for ethanol production: a review. Bioresource Technol. *83*, 1-11.

Takahashi, S. and Murata, N. (2008). How do environmental stresses accelerate photoinhibition? Trends Plant Sci. *13*, 178-182.

Thayer, S.S. and Björkman, O. (1992). Carotenoid distribution and deepoxidation in thylakoid pigment-protein complexes from cotton leaves and bundle-sheath cells of maize. Photosynth. Res. *33*, 213-225.

Townley-Smith, T.F., Depauw, R.M., Lendrum, Crystal, G.E. and Patterson, L.A. (1987). Kyle

Durum wheat. Can. J. Plant Sci. *67*, 225-227.

Tucker, C.J. (1979). Red and photographic linear combinations for monitoring vegetation. Remote Sens. Environ. *8*, 127-150.

Van Soest, P.J. and Wine, R.H. (1967). Use of detergent in the analysis of fibrous feeds. IV. Determination of plant cell wall constituents. J. Assoc. Offic. Anal. Chem. *50*, 50-55.

Vincent, J.H. et al. (1997). Reduced lignin content and altered lignin composition in transgenic tobacco down-regulated in expression of L-phenylalanine ammonia-lyase or cinnamate 4-hydroxylase. Plant Physiol. *115*, 41-50.

Wiegand, C.L., Richardson, A.J., Escobar, D.E. and Gerbermann, A.H. (1991). Vegetation indices in crop assessments. Remote Sens. Environ. *35*, 105-119.

Yang, X. Chen, X., Ge, Q., Li, B., Tong, Y., Zhang, A., Li, Z., Kuang, T. and Lu, C. (2006).Tolerance of photosynthesis to photoinhibition, high temperature and drought stress in flag leaves of wheat: A comparison between a hybridization line and its parents grown under field conditions. Plant Sci. *171*, 389-397.

Zeng, N., Qian, H. and Munoz, E. (2004). How strong is carbon cycle-climate feedback under global warming? Geophys. Res. Lett. *31*, 1-5.

7. APPENDIX

Page

Table A1- Photosynthetic data from weekly measurements on field-grown wheat in 2007. All measurements were taken under ambient, field conditions. Determined with portable reflectometers and fluorometer on newest fully-expanded leaf. Values represent means ± SD, (n=3).

	15-Jun-07			22-Jun-07		
Cultivar	**NDVI**	**F_V/F_M**	**PRI**	**NDVI**	**F_V/F_M**	**PRI**
Mckenzie	0.69 ± 0.02	0.73 ± 0.03	-0.33 ± 0.33	0.68 ± 0.02	0.74 ± 0.03	-0.28 ± 0.08
Glenlea	0.70 ± 0.01	0.72 ± 0.10	-0.35 ± 0.12	0.71 ± 0.02	0.76 ± 0.03	-0.33 ± 0.20
AC Crystal	0.71 ± 0.03	0.67 ± 0.03	-0.47 ± 0.36	0.70 ± 0.01	0.74 ± 0.01	-0.18 ± 0.13
AC Andrew	0.71 ± 0.01	0.76 ± 0.01	-0.42 ± 0.08	0.71 ± 0.01	0.76 ± 0.06	-0.22 ± 0.12
Superb	0.70 ± 0.01	0.73 ± 0.03	-0.62 ± 0.25	0.70 ± 0.03	0.76 ± 0.04	-0.21 ± 0.23
AC Vista	0.70 ± 0.03	0.76 ± 0.01	-0.37 ± 0.35	0.70 ± 0.02	0.72 ± 0.04	-0.18 ± 0.21
Snowbird	0.73 ± 0.01	0.74 ± 0.03	-0.55 ± 0.18	0.68 ± 0.03	0.73 ± 0.06	-0.19 ± 0.21
AC Barrie	0.72 ± 0.03	0.75 ± 0.01	-0.55 ± 0.17	0.70 ± 0.02	0.74 ± 0.01	-0.60 ± 0.42
5700 PR	0.73 ± 0.01	0.73 ± 0.04	-0.39 ± 0.26	0.68 ± 0.02	0.74 ± 0.04	-0.20 ± 0.08
Kyle	0.67 ± 0.04	0.71 ± 0.05	-0.29 ± 0.37	0.67 ± 0.04	0.73 ± 0.06	-0.22 ± 0.14
AC Avonlea	0.69 ± 0.04	0.76 ± 0.02	-0.33 ± 0.30	0.69 ± 0.03	0.73 ± 0.02	-0.26 ± 0.13
	29-Jun-07			**03-Jul-07**		
Cultivar	**NDVI**	**F_V/F_M**	**PRI**	**NDVI**	**F_V/F_M**	**PRI**
Mckenzie	0.72 ± 0.04	0.69 ± 0.08	-0.05 ± 0.14	0.73 ± 0.01	0.76 ± 0.01	-0.70 ± 0.20
Glenlea	0.73 ± 0.03	0.73 ± 0.06	-0.10 ± 0.09	0.73 ± 0.02	0.76 ± 0.02	-0.69 ± 0.29
AC Crystal	0.73 ± 0.02	0.69 ± 0.02	-0.17 ± 0.09	0.73 ± 0.01	0.75 ± 0.02	-0.72 ± 0.29
AC Andrew	0.71 ± 0.01	0.74 ± 0.08	-0.17 ± 0.19	0.72 ± 0.01	0.75 ± 0.04	-0.75 ± 0.42
Superb	0.74 ± 0.02	0.77 ± 0.01	-0.25 ± 0.09	0.73 ± 0.01	0.77 ± 0.01	-0.61 ± 0.39
AC Vista	0.72 ± 0.05	0.77 ± 0.03	-0.21 ± 0.03	0.72 ± 0.02	0.78 ± 0.01	-0.69 ± 0.31
Snowbird	0.72 ± 0.03	0.74 ± 0.05	-0.14 ± 0.16	0.70 ± 0.01	0.77 ± 0.02	-0.59 ± 0.43
AC Barrie	0.75 ± 0.01	0.76 ± 0.05	-0.28 ± 0.19	0.73 ± 0.01	0.73 ± 0.02	-0.73 ± 0.46
5700 PR	0.72 ± 0.02	0.76 ± 0.08	-0.16 ± 0.15	0.74 ± 0.01	0.78 ± 0.03	-0.58 ± 0.13
Kyle	0.70 ± 0.03	0.77 ± 0.01	-0.28 ± 0.05	0.69 ± 0.02	0.72 ± 0.06	-0.57 ± 0.41
AC Avonlea	0.72 ± 0.02	0.69 ± 0.09	-0.18 ± 0.14	0.72 ± 0.01	0.76 ± 0.02	-0.45 ± 0.21
	19-Jul-07					
Cultivar	**NDVI**	**F_V/F_M**	**PRI**			
Mckenzie	0.70 ± 0.02	0.7 ± 0.06	-0.68 ± 0.49			
Glenlea	0.72 ± 0.02	0.71 ± 0.08	-0.85 ± 0.43			
AC Crystal	0.69 ± 0.05	0.74 ± 0.02	-0.69 ± 0.45			
AC Andrew	0.74 ± 0.01	0.75 ± 0.01	-0.96 ± 0.69			
Superb	0.73 ± 0.02	0.76 ± 0.01	-0.96 ± 0.25			
AC Vista	0.70 ± 0.01	0.74 ± 0.01	-0.75 ± 0.25			
Snowbird	0.72 ± 0.04	0.70 ± 0.05	-0.96 ± 0.49			
AC Barrie	0.74 ± 0.01	0.73 ± 0.01	-0.84 ± 0.4			
5700 PR	0.73 ± 0.02	0.75 ± 0.01	-1.11 ± 0.15			
Kyle	0.70 ± 0.04	0.73 ± 0.01	-1.21 ± 0.13			
AC Avonlea	0.72 ± 0.04	0.74 ± 0.54	-0.76 ± 0.28			

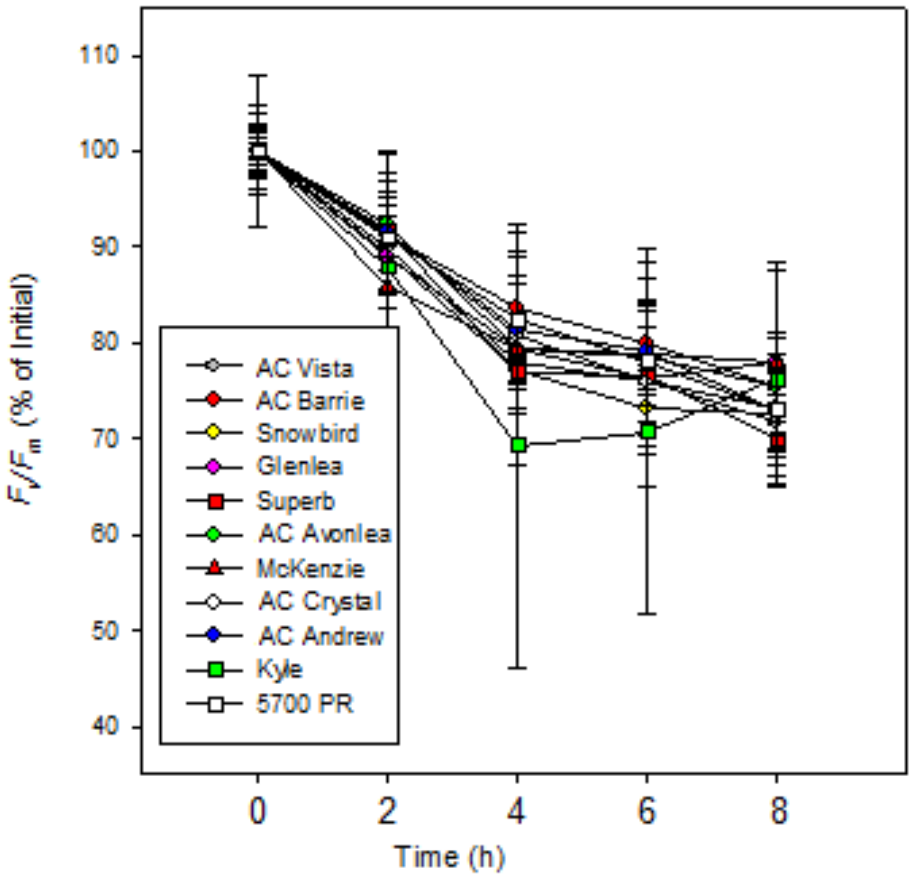

Fig A1- Photoinhibition curves of spring wheat cultivars from field-grown wheat in 2007. All measurements were taken at room temperature. Determined with chlorophyll fluorescence imaging on newest fully-expanded leaf. Values represent means ± SD, (n=3).

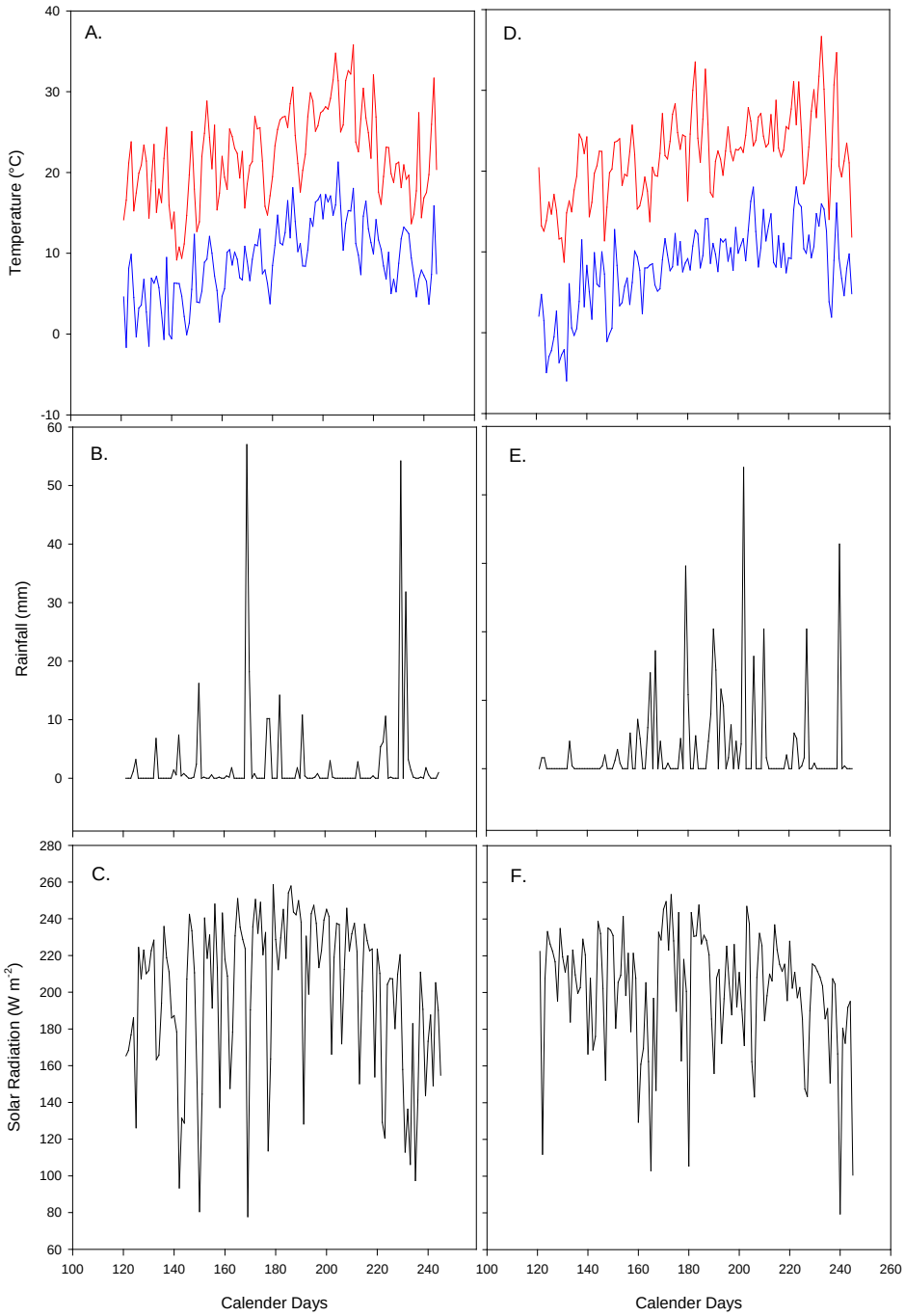

Fig A2- Meteorological data from 2007 and 2008 crop years. Data was obtained from Kernen Research Farm, Saskatoon SK. Data shown begins on May 1 and ends on September 1 in both growing seasons. Panels A-C and D-F show weather from 2007 and 2008, respectively.

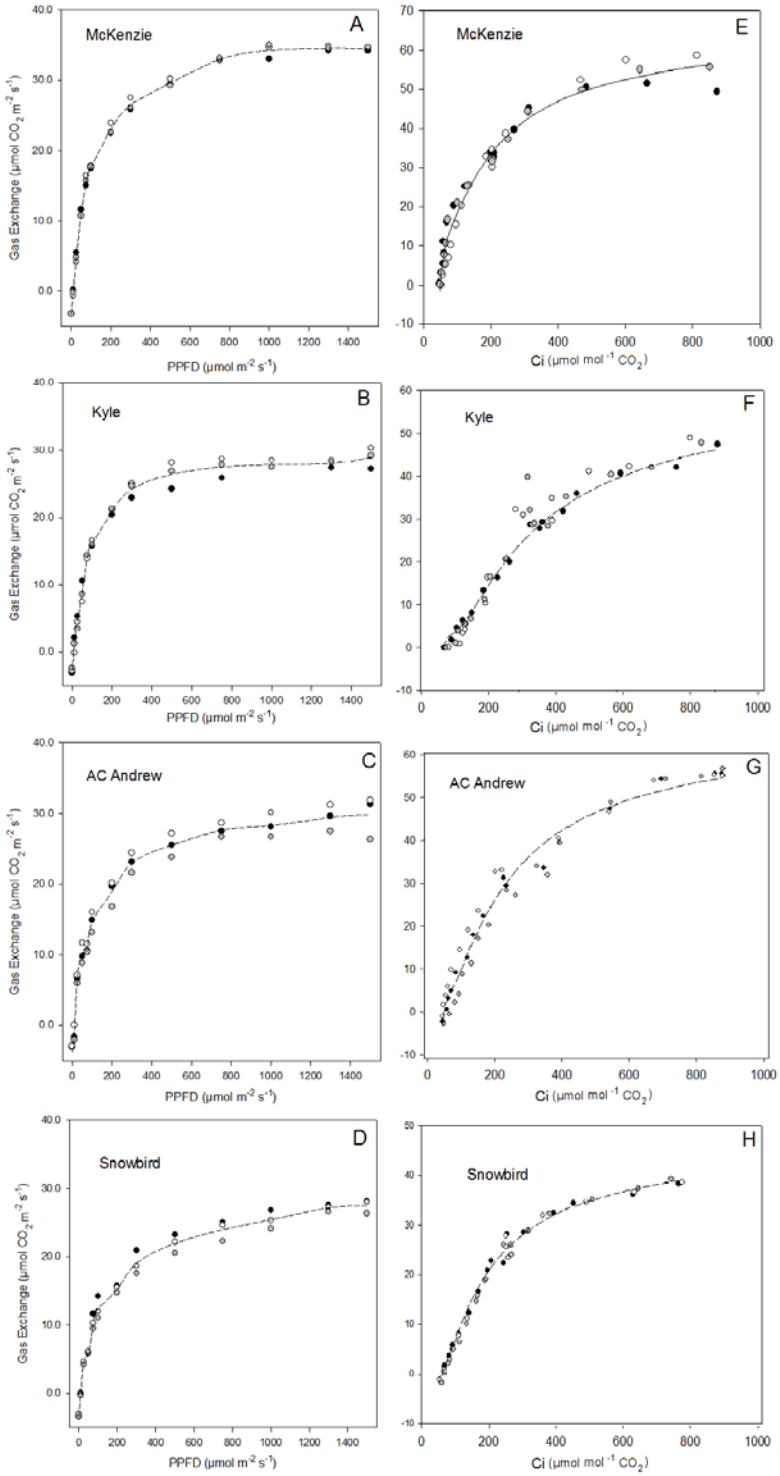

Figure A3-Light and CO_2 response curves from field-grown wheat grown in 2008 crop year. Panels A-D show light response curves while panels E-H show CO_2 response curves. Three replicates are shown with the average line of best fit.

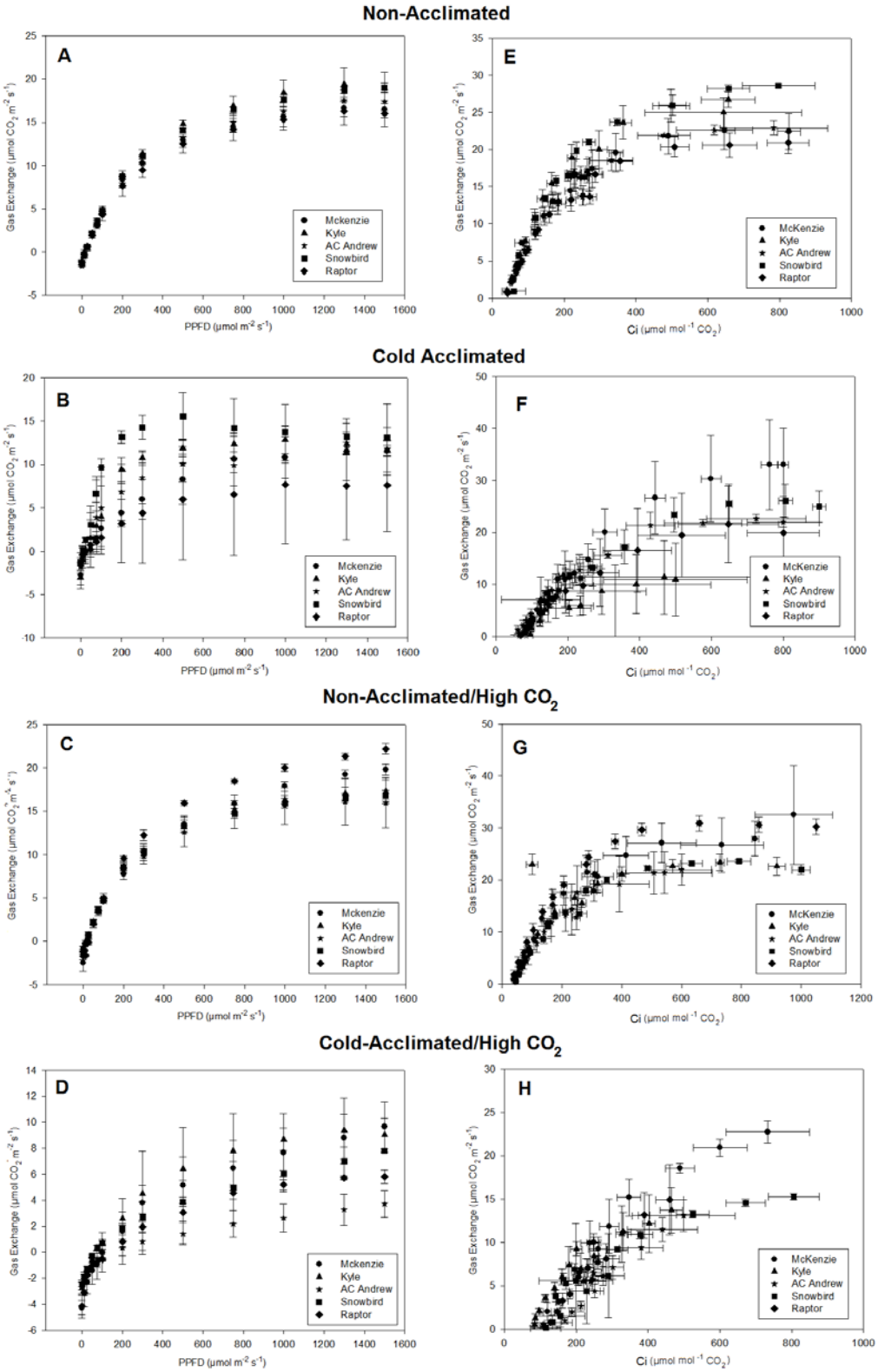

Figure B1- Light and CO_2 response curves from controlled environment studies. Panels A-D show light response curves while panels E-H show CO_2 response curves. Shown are means ± SD (n=3). When not present, error bars are smaller than symbol size.